Rhodes College Digital Archives - DLynx

Mechanisms of Ultrasonic Attenuation in Porous Bone

Item Type	Thesis
Authors	Milazzo, Stephanie
Publisher	Memphis, Tenn. : Rhodes College
Rights	Rhodes College owns the rights to the archival digital objects in this collection. Objects are made available for educational use only and may not be used for any non-educational or commercial purpose. Approved educational uses include private research and scholarship, teaching, and student projects. For additional information please contact archives@rhodes.edu. Fees may apply.
Download date	2025-07-16 02:53:23
Link to Item	http://hdl.handle.net/10267/13667

I give permission for public access to my Honors paper and for any copying or digitization to be done at the discretion of the College Archivist and/or the College Librarian.

Signed_____

Stephanie Michelle Milazzo

Date _____

Mechanisms of Ultrasonic Attenuation in Porous Bone

Stephanie Michelle Milazzo

Department of Physics
Rhodes College
Memphis, Tennessee

2012

Submitted in partial fulfillment of the requirements for the
Bachelor of Science degree with Honors in Physics

This Honors paper by Stephanie Michelle Milazzo has been read

and approved for Honors in Physics.

Dr. Brent Hoffmeister
Project Advisor/Department Chair

_____

Dr. Ann Viano
Second Reader

_____

Dr. Michael Sheard
Extra-Departmental Reader

_____

Acknowledgements

I would like to thanks Dr. Brent Hoffmeister for his mentoring in the lab and life plans for the past four years. The Physics Department (Dr. Brent Hoffmeister, Dr. Ann Viano, Dr. Deseree Meyer, Dr. Shubho Banerjee, Dr. David Rupke, Dr. Brentley Burnham, Mr. Glen Davis, Ms. Eva Owens) has been an incredible group to live and work among for four years, and I am extremely grateful for their teaching and support. The Physics Class of 2012 (Rebecca Miller, Anne Wilson, Nick Badger, Stan Badger, Brad Hensley, Jake Jackson, Michael Ethridge, Evan Nelsen) has been a wonderful group to journey alongside. In addition, lab collaboration with Jenna Smith, Anne Wilson, Morgan Smathers, and Joey McPherson has greatly helped me grow as a scientist.

Contents

List of Figures

List of Tables

Abstract

Mechanisms of Ultrasonic Attenuation in Porous Bone

by

Stephanie Michelle Milazzo

Ultrasound is a well established method for measuring the density of porous bone. Ultrasonic backscatter is one application of this technology. Backscattered power has been found to decrease with bone density. We hypothesized that increased attenuation causes a decrease in the backscattered power. There are two mechanisms of attenuation in porous bone: absorption and scattering of acoustic energy away from the forward direction. To determine the dominant mechanism for attenuation, we measured eight specimens of human and bovine bone ranging in density from 0.142-0.259 g/cc. Measurements were first performed with the specimens in water (with water filling the porous regions) and then in ethanol. By altering the saturating fluid, we altered the scattering properties of the bone, but not the absorption properties. We observed differences in the backscattered signals between water and ethanol measurement trials, but not between attenuation signals. This suggests that the dominant mechanism of attenuation is absorption.

Chapter 1: Introduction

SECTION 1.1: Osteoporosis

Osteoporosis is a major public health issue in the world today. Presently, four to six million women over the age of 50 worldwide have osteoporosis and thirteen to seventeen million women in the same category have osteopenia (a less advanced form of the disease). Annually in the United States, there are 250,000 hip fractures, 12-20% of which cause death from complications related to the fracture. Osteoporosis causes about 90% of hip and spine fractures in elderly women. To further complicate the matter, osteoporosis in its early stages has no symptoms. Diagnostic techniques to determine the onset and extent of osteoporosis in patients are necessary to help prevent osteoporotic fractures (Njeh at al, 13).

There are two types of bone tissue in the human body: cortical bone and cancellous bone. Cortical, or compact, bone is the bone comprising long, shaft-like portions of bones, surrounding a center of marrow. Cortical bone also forms a protective sheath around cancellous bone. Cancellous, or spongy, bone is composed of a three-dimensional array of branchlike structures called trabeculae. Spongy bone exists at the ends of long bones, near joints in the body. In addition, "cuboid" bones (such as vertebrae) are comprised of spongy bone surrounded by a cortical layer. Figure 1.1 shows the end of a long bone, with cancellous bone surrounded by a cortical layer.
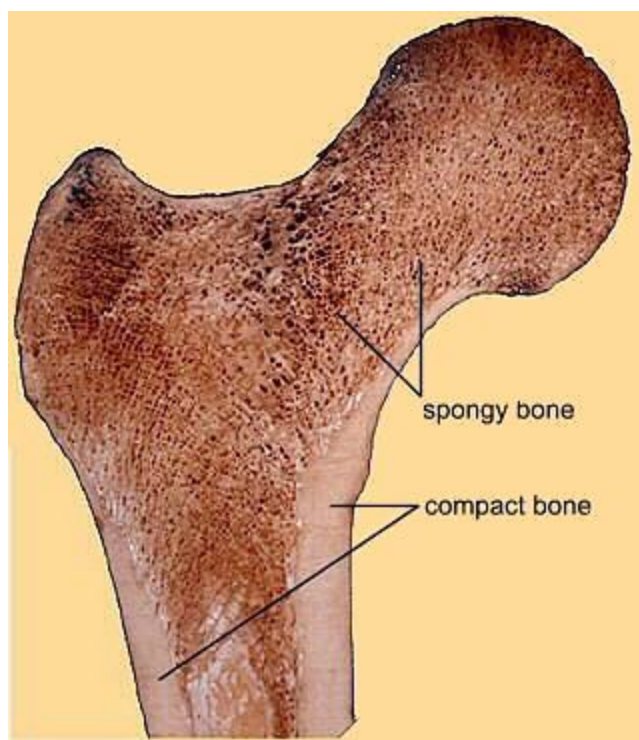
Figure 1.1: The end of a bone, consisting of a cancellous (spongy) bone interior in a cortical (compact) bone sheath.

Bone is consistently undergoing a process called remodeling. In normal bone life, two types of cells dominate the remodeling process of bone. These cell types, osteoclasts and osteoblasts, are responsible for the proper maintenance of bone. Osteoblasts build up new bone material, and osteoclasts tear down old bone material. This remodeling process occurs at the surface areas of bone, and serves to repair small fractures due to normal mechanical stress on bone. Because of the porous structure of cancellous bone, the surface area of cancellous bone is greater than that of cortical bone. As such, the effects of the remodeling process are more apparent in cancellous portions of bone.

In normal healthy bone, osteoclasts and osteoblasts function at similar rates, so there is no net loss in the bone mass. Degenerative bone disease, such as osteoporosis, occurs when there is an imbalance in the activity of the osteoclasts and osteoblasts.

Because of the higher surface area of cancellous bone, degenerative bone disease occurs first and more noticeably in the cancellous portions of bone. Figure 1.2 shows the difference between a normal and osteoporotic sample of human cancellous bone.
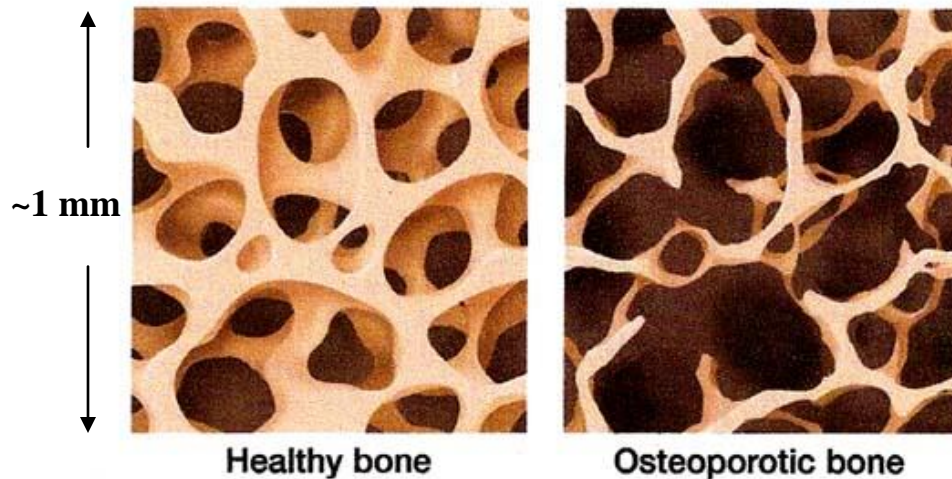
Figure 1.2: An image of a normal and osteoporotic section of human cancellous bone. Notice the decreased number and thickness of the trabeculae in osteoporotic bone.

Because bone disease is more pronounced in cancellous portions of bone, it is important to have bone density analysis techniques that can effectively measure density and density changes in the cancellous portions of bone. Many fractures caused by bone disease occur at cancellous bone regions in central skeletal sites, such as the hip and spine.

The standard technique for measuring bone density or bone density changes in central skeletal sites is dual energy X-ray absorptiometry (DXA). This method measures the bone mineral density (BMD) of bone. The decreased strength and density of osteoporotic bone causes changes in BMD. Osteoporotic bone can thus be distinguished from healthy bone by BMD deviation from that of healthy bone (Karjalainen, 13).

Although DXA is an effective method to measure bone density, there are numerous drawbacks to x-ray as a bone density analysis technique. The ionizing radiation delivered to patients by x-ray absorptiometry is a matter of concern. In addition, x-ray machines are large and not portable (see Figure 1.3). Also, x-ray diagnostic techniques are only effective at measuring bone mineral density, and are not sensitive to other qualities of bone, such as the collagen composition of bone. Because some bone diseases, such as osteogenesis imperfecta (brittle bone disease), are caused by a genetic collagen defect, diagnostic techniques sensitive to the composition of bone are necessary, making x-ray alone an inadequate bone diagnostic technique for this application.
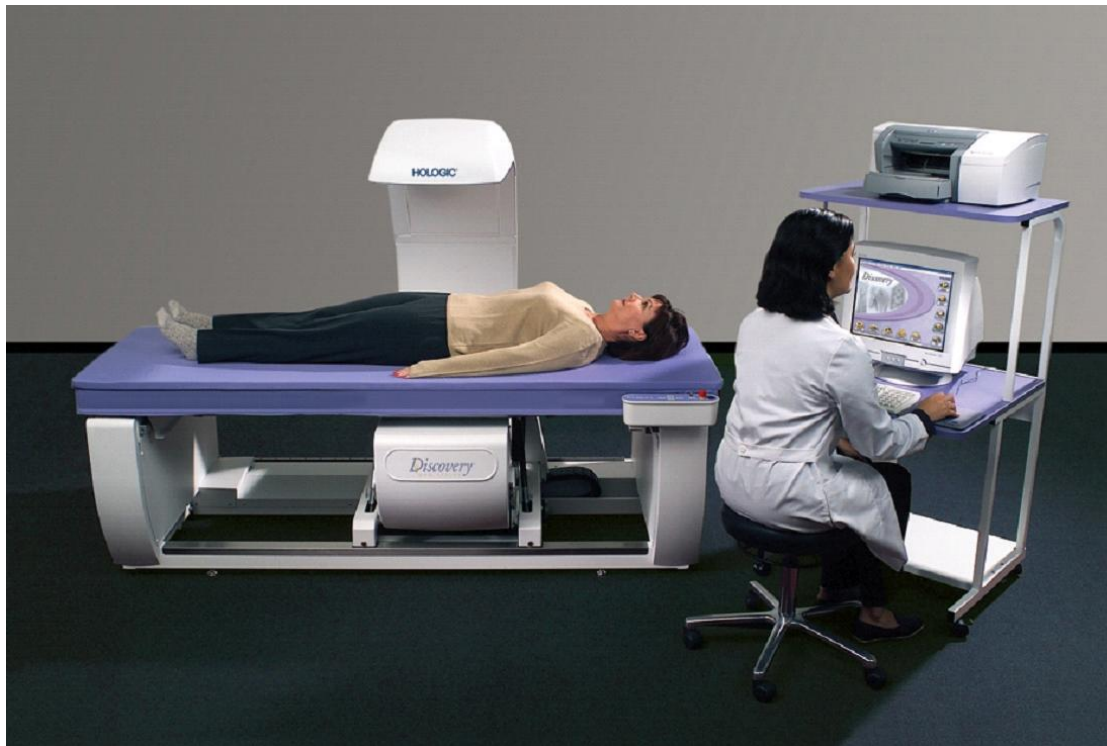
Figure 1.3: An example of an x-ray machine to measure bone density at central skeletal sites.

SECTION 1.2: Ultrasonic Techniques for Detecting Osteoporosis

Ultrasound offers an alternative method of clinical bone assessment. There are many benefits to using ultrasound instead of x-ray to assess bone health. Ultrasound lacks the ionizing radiation present in x-ray testing, ultrasonic machines are generally less expensive and more portable than their x-ray counterparts, and the interaction of the ultrasonic beam with the bone tissue could reveal more properties than just density, such as the mineral and collagen composition of bone.

The use of ultrasonic tests to measure bone density are based upon the principle that ultrasonic wave propagation will change with changing physical characteristics of bone. The bone density changes in composition and microstructure caused by osteoporosis can therefore be quantified by ultrasonic measurement techniques.

Currently, the primary methods for bone testing with ultrasound involve through-transmission procedures, in which an ultrasonic transducer is placed on one side of the bone, and an ultrasonic receiver is placed on the other side of the bone. The loss in signal intensity and change in wave speed are measured and used to analyze the density of the bone specimen. The through-transmission measurement technique is shown in Figure 1.4.
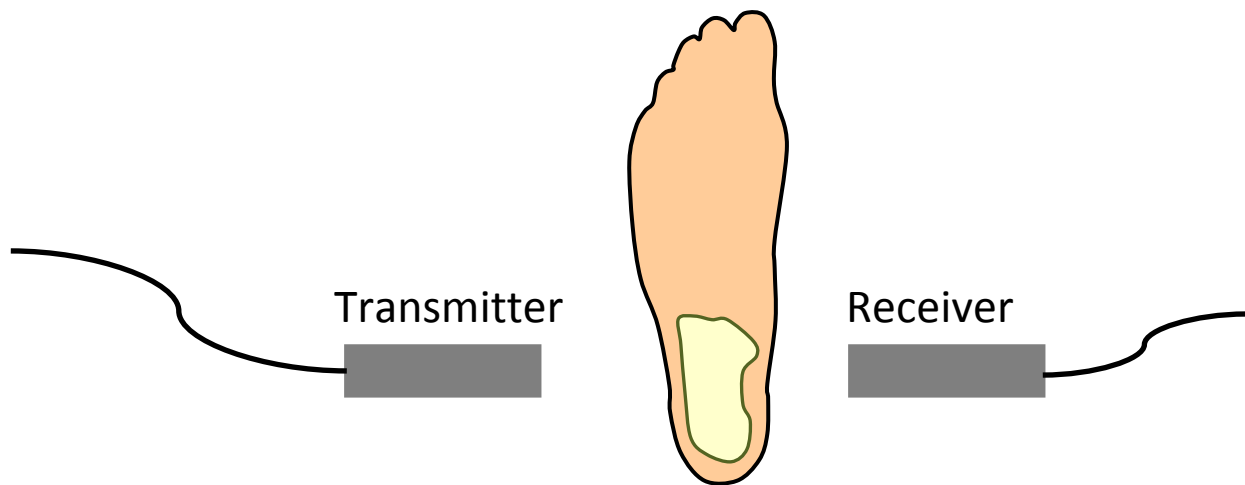
Figure 1.4: Illustration of the procedure for through-transmitted ultrasound measurement at the heel. A transducer is placed on one side of the bone and a receiver on the other. An ultrasonic signal is transmitted by the transducer, interacts with the bone, and is received on the other side by the receiver. The attenuation in the signal can be analyzed and correlated to bone density. Clinically, such measurements are often performed at the heel.

In through-transmission, the speed of sound is measured by comparing the time of flight of the ultrasonic pulse through the bone and through water. The differences between these times of flight can be used to determine the speed of sound through the bone tissue. The speed of ultrasonic waves in cancellous bone correlates with bone density.

Another important parameter analyzed by through-transmission ultrasonic techniques is attenuation of ultrasound. The attenuation of the ultrasonic signal is the loss of ultrasonic power as the signal propagates through the bony material. Cancellous bone is very attenuating, due to the irregular structure and its high density. Higher density bone attenuates ultrasound more strongly than lower density bone. Thus, attenuation techniques can be used to assess bone density.

Through-transmitted techniques can only be used at peripheral sites of the body, such as the heelbone (see Figure 1.5). However, since many osteoporotic fractures occur at central skeletal sites, such as the hip and spine an ultrasonic measurement system which can measure bone density at these places is desirable. In addition, bone density changes that occur due to bone disease occur first and more strongly in cancellous bone. The hip and spine have a high volume fraction of cancellous bone.

Figure 1.5: A typical ultrasonic measurement system to analyze the density of a heelbone using through-trasmitted ultrasound.

To measure central skeletal sites using ultrasound, a new technique using ultrasonic backscatter has been proposed. In this technique, a single ultrasonic transmitter is placed on one side of a bone. An ultrasonic signal is transmitted into the bone and interacts with the trabeculae in the cancellous bone. The signal is scattered in many

directions every time it encounters an interface, and the portion that is scattered back to the ultrasonic transmitter is measured as the backscattered signal (Njeh, 399). This process is shown in figure 1.6. A portion of the signal in the time domain is chosen for analysis, typically a portion representing part of the interior of the bone specimen. This signal can be correlated with bone density to analyze density and density changes in bone at central skeletal sites. Density changes in bone are caused by changes in the composition of bone material and changes in the bone's microstructure (number and size of trabeculae).

The scattering properties of trabeculae are dependent upon the geometry of the trabeculae and the acoustic impedance mismatch between the trabeulae and the surrounding fluid. Acoustic impedance is a measure of the acoustic propagation through the bony material (acoustic impedance $Z = c\rho$, where c is the speed of sound in the material and ρ is the density of the material). So, the scattering of the ultrasonic waves by the trabeculae is dependent upon the acoustical properties of the trabeculae and the surrounding medium.
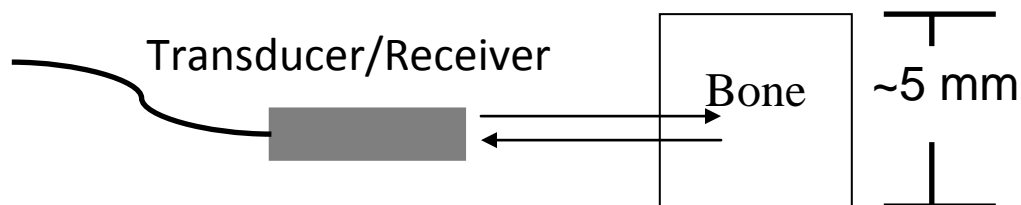
Figure 1.6: A schematic for the backscattered ultrasound analysis technique. A single ultrasonic transducer/receiver is placed on one side of the bone specimen, the signal interacts with the bone specimen, and the portion of the signal scattered directly back to the transducer is analyzed.

Previous work investigated several parameters based on ultrasonic backscatter, some of which show strong promise for clinical relevance. For example, Apparent Integrated Backscatter (AIB), which measures the average power returned from the bone over a chosen frequency bandwidth, has shown good correlation with bone density. Also, the Frequency Slope of Apparent Backscatter (FSAB), which describes the frequency dependence of the backscattered power (the slope of the power scattered back versus frequency), has shown some diagnostic promise. Most of these studies have been performed at frequencies over 1 MHz.

AIB, has been found to decrease with increased bone mineral density (Hoffmeister, Whitten, and Rho 635-642, Hoffmeister, Jones, Caldwell, and Kaste 2715-2727, Hoffmeister, Johnson, Janeski, Keedy, Steinert, Viano and Kaste 1442-1452). This finding has been somewhat surprising, because intuitively denser bone should reflect back more sound to the transducer. But, the high attenuation of high density bone specimens may be a more dominant effect.

There are two main mechanisms of attenuation of ultrasonic signals in cancellous bone: scattering and absorption. Scattering occurs when sound is scattered away from the forward propagation direction by interaction with the bone's trabeculae. Absorption occurs when the sound is converted from acoustic energy to heat while propagating through the bony material. The effects of both of these mechanisms increase with increasing bone density, because of the increased number and thickness of the trabeculae in the cancellous bone.

It is unknown at this point whether absorption or scattering is the dominant mechanism of attenuation in cancellous bone. The relative contributions of these two

mechanisms are important to understanding the interaction of the ultrasonic signals with cancellous bone, and how these interactions depend on bone composition and microstructure.

SECTION 1.3: Previous results of absorption versus scattering

The relative contributions of absorption and scattering to signal attenuation in cancellous bone have been explored to a limited extent. Keith Wear found in a study on backscatter and attenuation that backscattered power varies as frequency to the third power, while attenuation varies as frequency to the first power. This result indicates that absorption could be a dominant mechanism of attenuation. If scattering were the dominant mechanism of attenuation, it would cause attenuation to vary as frequency cubed as well (Wear, 2000). These findings were taken in the 500 kHz range of ultrasound in human calcaneus (heelbone).

Another study to validate this finding was conducted in 2000 by S. Chaffai and V. Roberjot. Their study was also conducted on human calcanae in the frequency range 0.4-1.2 MHz. These findings agree with the findings of Wear that absorption is the dominant mechanism of ultrasonic attenuation in cancellous bone (Chaffai and Roberjot, 2000).

A very recent study was conducted in 2011 by K. Li II and M.J. Choi in the 0.2-1.2 MHz range on bovine cancellous bone, comparing the frequency dependence of attenuation and scattering. They also found absorption to be the dominant mechanism of attenuation by comparing the frequency dependence of the absorption and scattering in the bone. However, this group also speculated that scattering may become a more

important factor in the attenuation of the ultrasonic signal at frequencies higher than 0.6 MHz (Li and Choi, 2011).

Other studies have suggested that scattering is the dominant mechanism of attenuation. A simulation study of ultrasonic propagation through cancellous bone in the frequency range 300-900 kHz found that scattering was more important than absorption (Kaufman, Luo, and Siffert, 2003).

SECTION 1.4: Objective of this Project

There is clearly a lack of consensus in the literature about the relative contributions of absorption and scattering to attenuation in cancellous bone in any frequency range. In addition, there are no experimental data in a higher frequency range of ultrasound (~4-6 MHz), necessitating further work to expand the current findings on attenuation in cancellous bone to that frequency range. The goal of this study was to determine the relative contributions of absorption and scattering in cancellous bone in the frequency range 1-6 MHz, and to identify the dominant mechanism of attenuation. To do this, it was necessary to isolate the effects of the two mechanisms to determine which is more significant.

To accomplish this, the properties of the bone were analyzed using ultrasonic backscatter with the porous portions of the bone filled with water and alcohol. Changing of the filling fluid of the bone specimens should alter the scattering properties of the bone but not the absorption properties. Water and alcohol were chosen for this study because they are significantly different in their acoustic impedance, but similar in their acoustic attenuating properties (both essentially have zero acoustic attenuation). Because of this,

the change in scattering properties between alcohol and water saturated bone should be significant. The physical material of the bone has not changed, so the absorption, or conversion of acoustical energy to heat by the bone material, will not change either. However, the acoustic impedance mismatch between the bone and surrounding fluid will have changed, making the scattering properties of the bone change as well.

Thus, by altering the filling fluid of the pores of the bone, we have isolated and altered the scattering properties of the bone and kept the absorption properties the same. In this way, we will be able to isolate the effects and importance of the two mechanisms of attenuation: absorption and scattering.

Chapter 2: Materials and Methods

SECTION 2.1: Specimen Preparation

The bone specimens used in this study were prepared from human femurs and bovine tibiae. The neck of the femur (the hip) is a common site of osteoporotic fractures and thus clinically interesting and relevant for our study. The bovine tibia provide a similar portion of bone, but, since bovine bones are denser, allow experimentation over a wider range of bone densities. These bones were sectioned into pieces approximately 5 mm x 15 mm x 15 mm (see Figure 2.1). The larger faces on the slices are perpendicular to the lateral and medial orientation on the bone (towards and away from the central long axis of the body), because measurement of bones in the human body using backscatter would likely be performed in these orientations. For experimental convenience, the marrow in the pores of the bone was removed using a Waterpik and the specimens were stored in a saline solution for preservation before and between ultrasonic tests.

Figure 2.1: Two specimens of cancellous bone in slices approximately 5 mm x 15 mm x 15 mm.

SECTION 2.2: Density Measurements

The density of the specimens was determined by dividing the mass of each specimen by the volume. The volume of the bone specimens was measured using calipers at several sites on the bone specimen. The length and width were measured at 3 sites each: the 2 edges and the middle of each side, as indicated in Figures 2.2 and 2.3. The thickness of each specimen was measured at five sites: each of the four corners and the center, as shown in Figure 2.4.
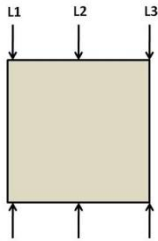
Figure 2.2:
Measurements
of length
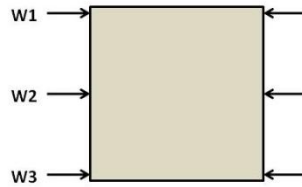
Figure 2.3:
Measurements
of width
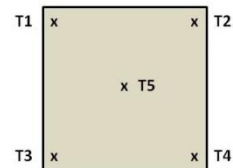
Figure 2.4:
Measurements
 of thickness

To determine the volume of each specimen, the length, width, and thickness measurements were each averaged. From these averaged values, the volume was calculated.

To measure the dry mass of each specimen, compressed air was used to remove most of the excess liquid in the bone. The specimens then were left to air dry at room temperature. The masses of the specimens were measured periodically over a period of 28 hours to ensure that the specimens had completely dehydrated. After about 4 hours, the mass of the specimens stabilized, as demonstrated in Figure 2.5.
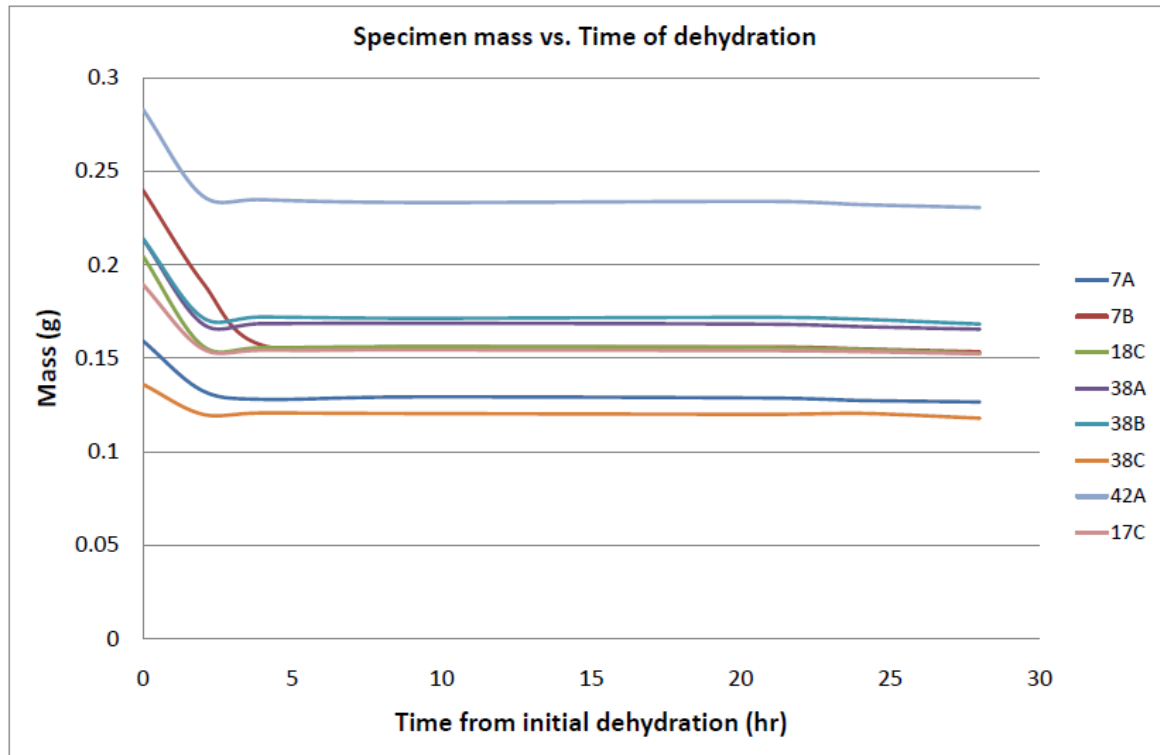
Figure 2.5: Measured mass of bone specimens over a period of 28 hours. Maximum dehydration is reached around 4 hours.

SECTION 2.3: Ultrasonic Testing

As described earlier, this study measures the ultrasonic properties of cancellous bone saturated with water or alcohol. In total, four tests were performed on each specimen in the order water, alcohol, water, alcohol, with each subsequent test being about two weeks after the last. Each test was performed in a bath of the appropriate fluid at room temperature. To ensure that the fluid was filling the pores of the bone sufficiently, the saline solution was removed from the specimen using compressed air. Then, the specimen was degased in the appropriate fluid under a vacuum pump for ten minutes, to ensure saturation of the fluid through the pores of the bone.

The specimen was placed on a custom mechanical stage designed to allow the simultaneous measurement of attenuation and backscatter. The specimen was supported by two thin steel prongs about a centimeter above a polished, level, steel reflector plate. The ultrasonic transducer (which functions as both a transmitter and receiver) was placed one focal length above the front surface of the bone specimen. This is shown in Figure 2.6.

Transmitter/
Receiver

Bone specimen
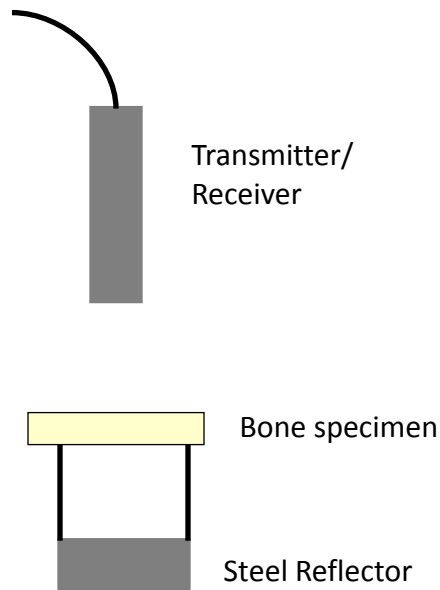
Steel Reflector

Figure 2.6: The measurement system for backscatter and attenuation in the cancellous bone. The bone specimen is propped above a smooth steel reflector, with the ultrasonic transducer one focal length above the front surface of the specimen. This whole setup would be immersed in the fluid at room temperature for testing.

A mechanical scanner was used to move the ultrasonic transducer to measure a 1 cm x 1 cm region of interest (ROI), which corresponds to a 100x100 point scan centered on the center of the face of the bone specimen. Tests were performed on both the lateral and medial sides of the bone specimen (top and bottom in Figure 2.6). 10,000 ultrasonic signals were obtained and averaged through each side of each specimen in each liquid

trial. So, in total, 80,000 ultrasonic tests were performed on each specimen over the course of the experiment.

The transmitter/receiver was a 5 MHz piezoelectric transducer, positioned one focal length above the front surface of the specimen. This focal length was different in water and alcohol, due to the different speeds of sound in the two fluids.

The transducer was first positioned at one focal length above the bone specimen, and then a reference signal for through-transmission measurements was acquired from the steel reflector with the specimen removed. This reference signal is used in analysis to compare the relative strengths of the attenuated signals to signals that have not propagated through bone.

The through-transmitted signal was measured as the portion of the signal that passes through the bone, reflects off of the steel plate, passes through the bone again, and is received by the ultrasonic transducer above the bone, as demonstrated in Figure 2.7. This signal has attenuated significantly upon passing through the bone twice, but the narrow thickness of our specimens allows a detectable signal to pass through.

Transmitter/

Receiver

Transmitted

Through-transmitted

Bone specimen
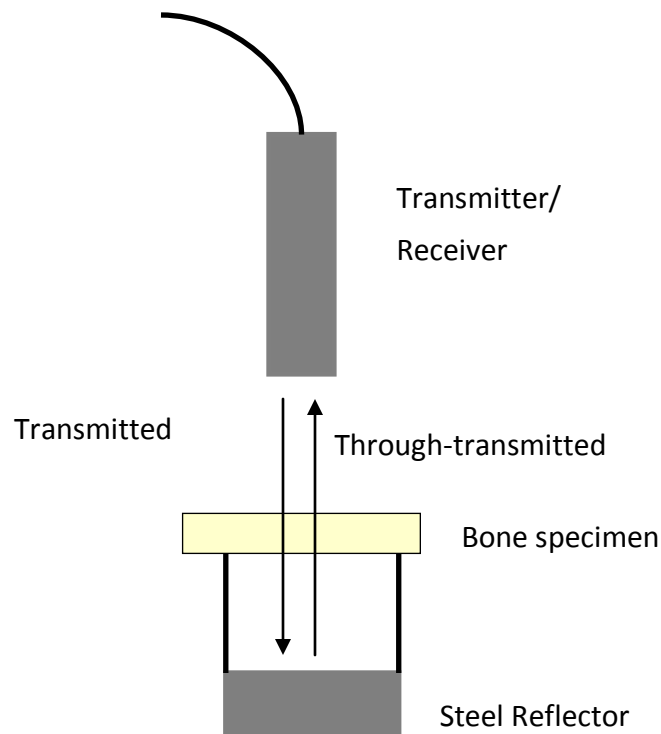
Steel Reflector

Figure 2.7: The through-transmitted signals pass through the bone specimen, reflect off of the steel reflector, and are transmitted back through the bone specimen to the ultrasonic transmitter/receiver.

Another reference signal was obtained for the backscatter measurements with the ultrasonic transmitter/receiver positioned one focal length above the steel reflector. The power spectrum is compared to that of the backscattered signal.

The backscattered ultrasonic signal was measured from the interior of the bone specimen as the signal passes through the bone.

SECTION 2.4: Speed of Sound Measurements

To accurately compare ultrasonic backscatter values from water- and alcohol-saturated bone specimens, the same physical regions of the bone should be analyzed. In order to choose appropriate portions of the backscatter signal in the time domain to analyze, the speed of sound in water- and alcohol-saturated bone must be measured. The

speed of sound through cancellous bone with the two different saturating fluids was calculated using the through-transmitted signals. The beginning of the pulse was found using a "time zero" analysis technique. In this method, a signal analysis program finds the maximum amplitude of the portion of the signal in the time domain specified by the user as "noise" (typically at least 1 μs of noise was recorded before the pulse). After finding this, the program finds the "time zero" of the signal pulse, or when the absolute magnitude of the signal deviates from zero by more than the absolute magnitude of the noise. This process is shown in Figure 2.8. The time zero is calculated for both the reference signal and the specimen signal. The ultrasonic probe is not moved between these measurements, so any deviations of the position of the signal in the time domain are caused by the difference of acoustic path length caused by the addition of the cancellous bone in the sound path. This time difference depends on the speeds of sound in the surrounding fluid and speed of sound in cancellous bone saturated with the surrounded fluid. The speed of sound in the fluid alone is known as a function of the temperature, as shown in Equations 2.1 and 2.2 below. From this information, the speed of sound in the cancellous bone with different saturating fluids can be calculated.

$$c_{water} = 1402.73 + 5.03358T - 5.79506 \times 10^{-2} T^2 + 3.31636 \times 10^{-4} T^3 \\ - 1.4562 \times 10^{-6} T^4 + 3.0449 \times 10^{-9} T^5$$

2.1

where the Temperature T is in degrees Celcius. (Slutsky, L.J.)

$$c_{alcohol} = 50(0.66) + 2663.73851 - 6762.56551T + 2921.22328T^2$$
$$+ 18073.7580T^3 - 30701.7452T^4 \qquad\qquad 2.2$$

where the Temperature T in degrees Kelvin. (Khasanshin, T.S. and A.A. Aleksandrov)
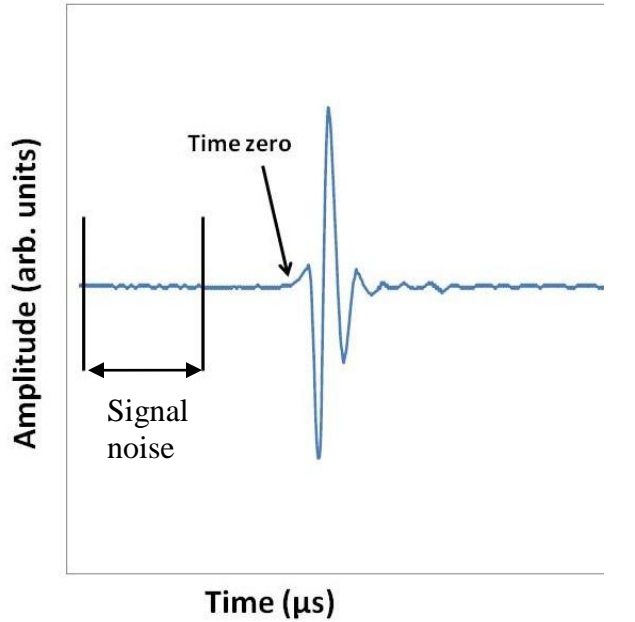
Figure 2.8: A user-specified gate of signal noise is analyzed for the maximum absolute amplitude of noise. The time after this gate in which the signal amplitude is first greater than the maximum amplitude of noise is specified as the "time zero" of the signal, or where the ultrasonic pulse begins.

SECTION 2.5: Backscatter Measurements

To analyze the backscatter signals, certain portions of the measured signals are gated for analysis. In each case, the length of the gate, τ_L, is the equivalent of 2.97 mm of total signal travel. In water, this corresponds to a signal length of 2 μs, and for alcohol, this corresponds to a signal length of 2.47 μs. For the reference signal, the analysis gate is centered about the peak of the signal, and in the backscattered signal, the gate is delayed by a specified amount, τ_D. This delay is used to exclude the echo from the front surface of

the specimen. Figure 2.9 shows these two distances. This flat surface of exposed

cancellous bone does not occur in the human body, so it is of no clinical relevance. The

delay was chosen to be three times the duration of the pulse returned from the polished

steel reflector. This corresponded to a gate delay of 1.98 µs in water and 2.45 µs in

alcohol. The beginning of the signal was determined by a thresholding algorithm in

which the absolute maximum of the signal was found. The thresholding algorithm found

the earliest point in the time domain at which the signal deviated from the zero power by

a user-specific percentage of the power value of the absolute maximum of the signal. For

our analysis, we defined this threshold as 20% of the absolute maximum.

Backscatter Signal
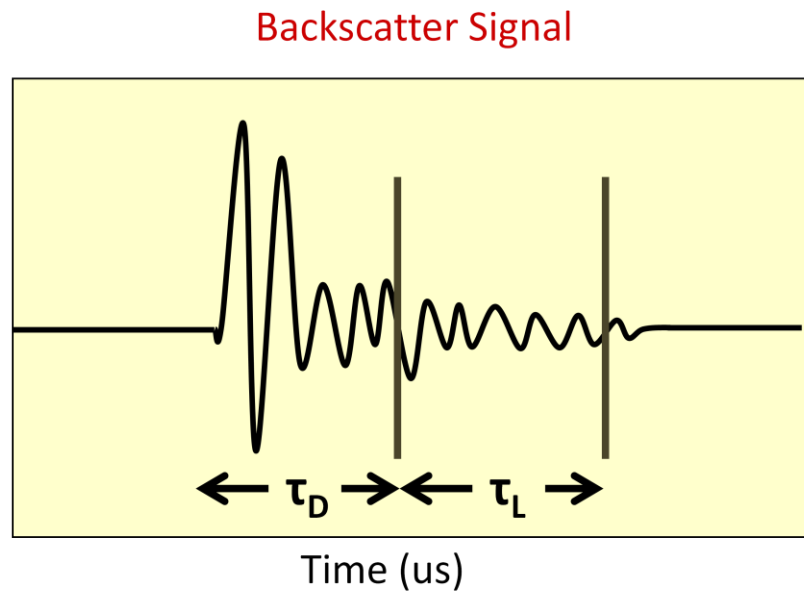
Figure 2.9: The front surface signal is avoided by delaying the signal gate by time τ_D. The portion of the signal to be analyzed is labeled τ_L.

A Fourier transform is performed on the gated portion of the calibration signal

and the specimen signal at each site in the region of interest on the bone, as shown in

Figure 2.10. At each site, the reference, or calibration, frequency spectrum is subtracted

from the backscattered spectrum, giving a function of power backscattered from the bone

as a function of frequency. This function is called the Apparent Backscatter Transfer Function, or ABTF. This process is shown in Figure 2.11.

After the Apparent Backscatter Transfer Function is calculated, a linear fit is performed over the chosen frequency bandwidth (see Figure 2.12). The process for bandwidth selection is described in Section 2.7. Several parameters are calculated from this linear fit and later will be analyzed in comparison to bone density for clinical relevance. The average power of the ABTF over the specified bandwidth is calculated as the Apparent Integrated Backscatter, or AIB, and is measured in dB. The slope of the linear fit is also calculated, and defined as the Frequency Slope of Apparent Backscatter, or FSAB, and measured in dB/MHz. Finally, the intercept of the linear fit with the power axis is calculated and defined as the Frequency Intercept of Apparent Backscatter, measured in dB.

Each of these parameters are calculated at each site of the bone specimen and averaged over the specified region of interest of bone (in our case, this was a 100 point by 100 point square in the center of the specimen, 1 cm by 1 cm, giving an average of 10,000 values for each of the parameters). Each parameter is then graphed versus apparent specimen density. These results will be discussed in Chapter 4.
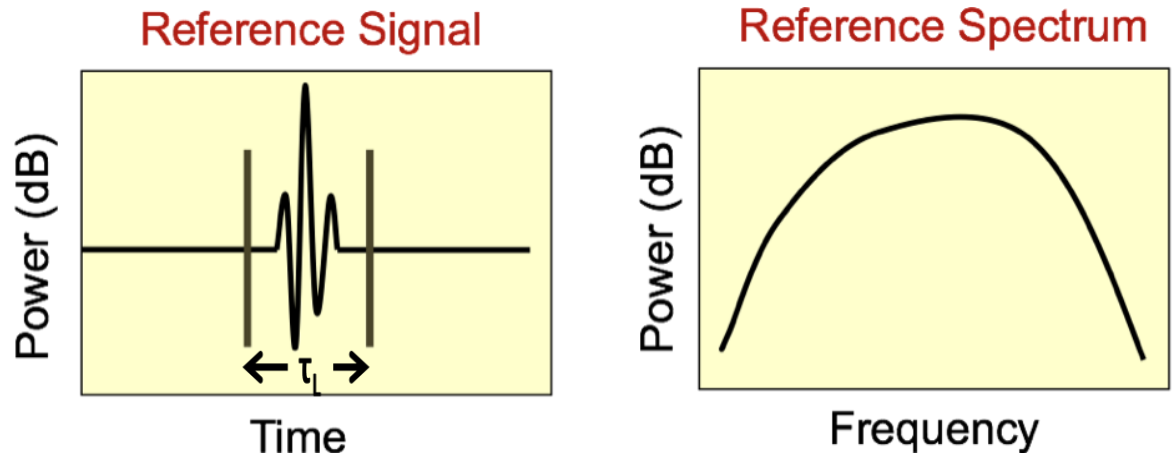
Figure 2.10(a): Fourier transform of a reference signal used for backscattered measurements. The frequency spectrum of the signal is relatively smooth, with a peak around the center frequency of the transducer: 5 MHz in our case.
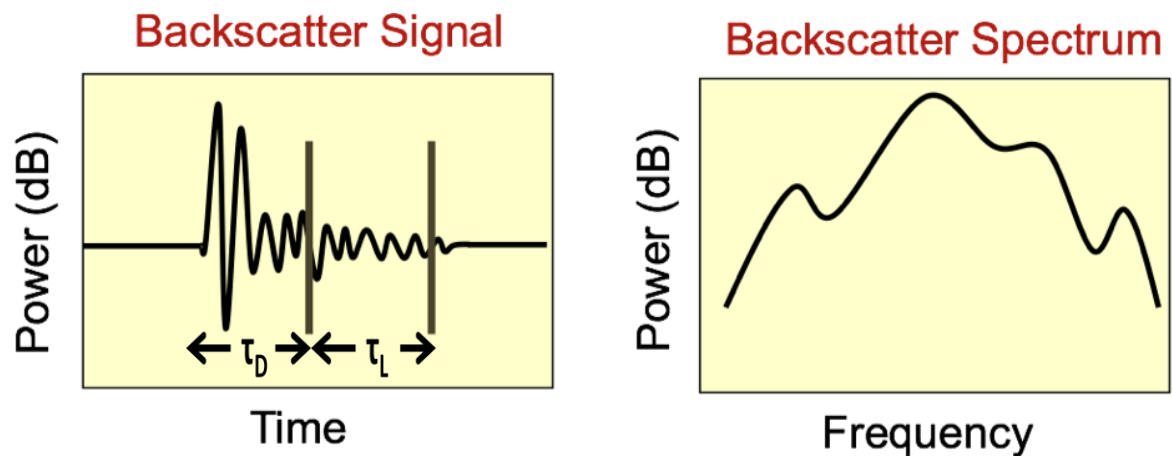
Figure 2.10(b): Fourier transform of a gated portion of a backscattered signal. The frequency spectrum is much less smooth than that of the reference spectrum, due to inhomogeneities in the trabecular bone structure.
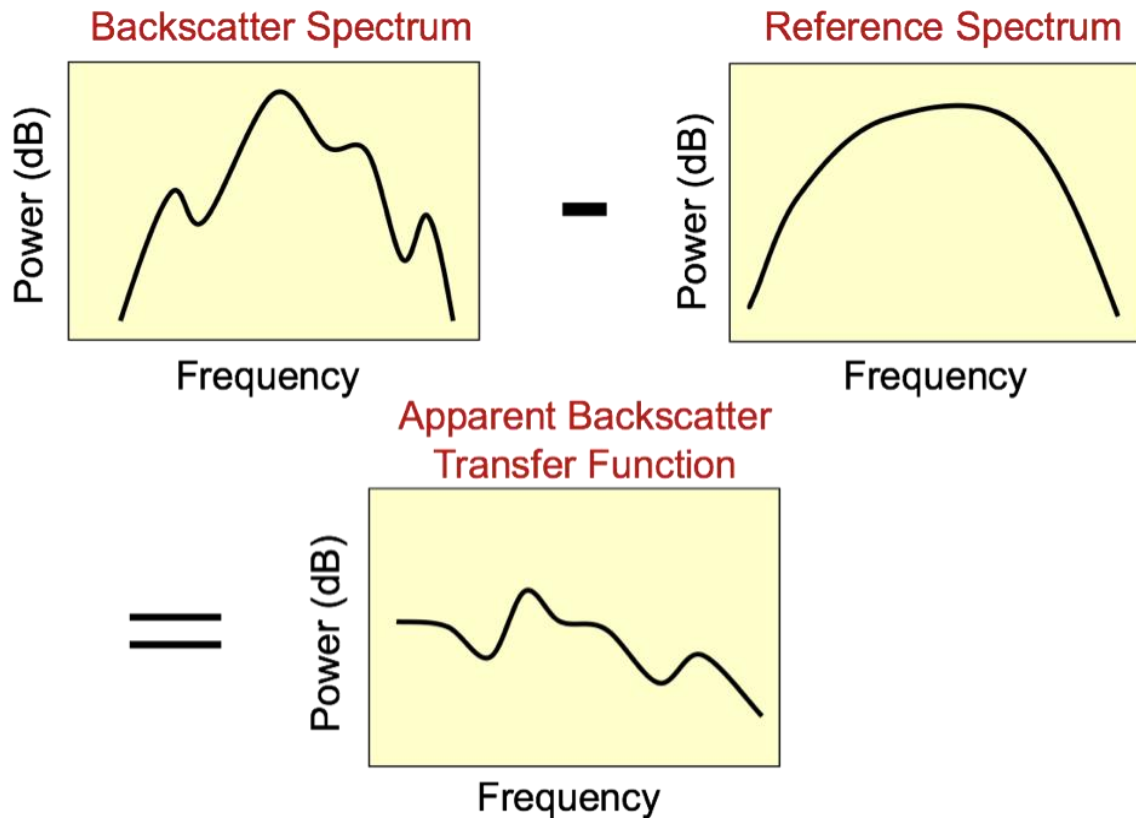
Figure 2.11: The Apparent Backscatter Transfer Function is found by subtracting the Fourier transform of the gated portion of the reference signal from the Fourier transform of the gated portion of the backscattered signal. The ABTF represents the backscattered power from the specimen corrected for the frequency dependent characteristics of the transducer and measurement system.

Apparent Backscatter Transfer Function
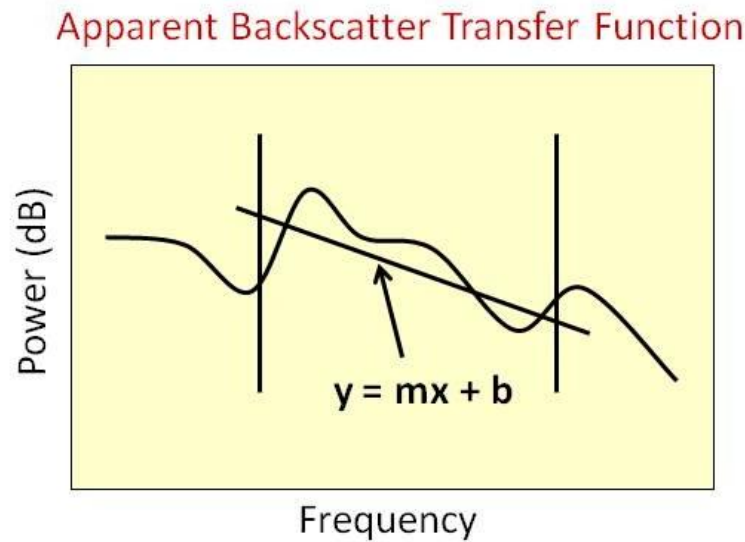
Figure 2.12: A linear fit is performed on the appropriate bandwidth of the Apparent Backscatter Transfer Function. The Apparent Integrated Backscatter (AIB) is defined as the average power backscattered over the specified frequency range, the Frequency Intercept of Apparent Backscatter, and Frequency Slope of Apparent Backscatter (FSAB) is defined as the slope of the linear fit ("m" in this image).

SECTION 2.6: Attenuation Measurements

To analyze the attenuation of the bone specimens, the signal reflected from the steel plate reflector after transmission through the bone was compared to a signal acquired from the steel plate alone. The attenuation analyzed is thus effectively the attenuation of a bone sample twice the actual thickness of our specimens, due to the attenuation caused on the way to and back from the steel reflector.

The portion of signal in the time domain to analyze is chosen to be the same length, τ_L, as the analysis gates for backscatter analysis. These lengths are 2 μs in water and 2.47 μs in alcohol. Since the reference and specimen signal for the attenuation measurements consist of one ultrasonic pulse, the analysis gate is centered on the signal. This is accomplished by taking the absolute value of the signal and centering the gate on the absolute maximum of the signal.

A Fourier transform is performed on the shadowed reference signal and the reference signal, as demonstrated in Figure 2.13. The shadowed reference spectrum is subtracted from the reference spectrum and the resulting spectrum is defined as the Signal Loss Transfer Function, which demonstrates the attenuating effects of the bone as a function of the signal frequency. This function is shown in Figure 2.14.

Parameters measuring the attenuating effects of the bone are then calculated from the Signal Loss Transfer Function over an appropriate bandwidth (the choice of this bandwidth is described in Section 2.7). A linear fit is applied over the selected bandwidth. The Frequency Averaged Attenuation, or FAA, is the average power value of the Signal Loss Transfer Function divided by twice the thickness of the bone sample. This measurement gives a value for power loss per cm of bone encountered, measured in dB/cm. The Broadband Ultrasonic Attenuation, or BUA, is the slope of the linear fit of the Signal Loss Transfer Function over the specified bandwidth divided by twice the specimen thickness, measured in dB/(MHz cm). The calculation of these parameters is shown in Figure 2.14. The division of each parameter by twice the specimen thickness serves the purpose of normalizing the attenuating properties of the bone by the thickness of the bone. The factor of two is due to the signal being transmitted through the bone to and from the reflector, so the attenuating effects of the bone occur through twice the bone thickness.

Reference Signal

Reference Spectrum
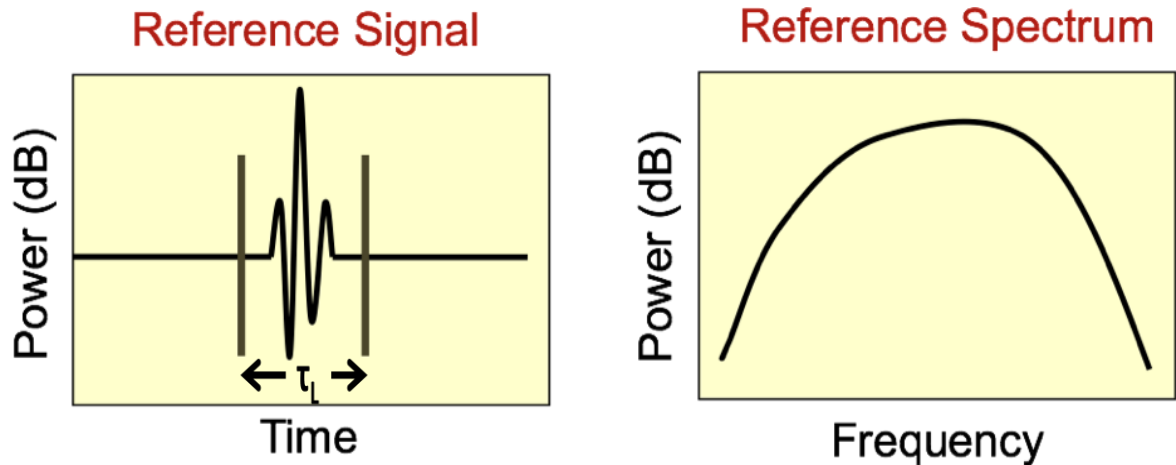
Figure 2.13(a): A Fourier transform is performed on a reference signal acquired from the steel reflector plate with no specimen over the steel plate. The spectrum obtained is a smooth curve centered near the center frequency of the transducer, in our case, 5 MHz.

Shadowed Reference Signal

Shadowed Reference Spectrum
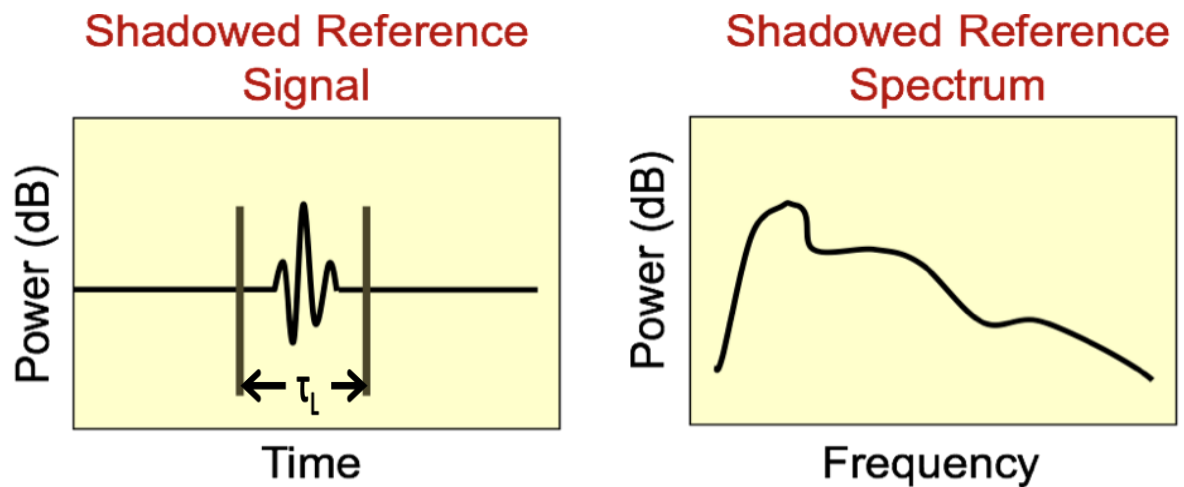
Figure 2.13 (b): A Fourier transform is performed on the shadowed reference signal acquired from the steel plate. This signal has passed through the bone specimen twice before being received back by the ultrasonic probe. The frequency spectrum is irregular due to structural irregularities in the bone. It has also shifted down in the frequency spectrum, due to higher attenuation of higher frequencies.
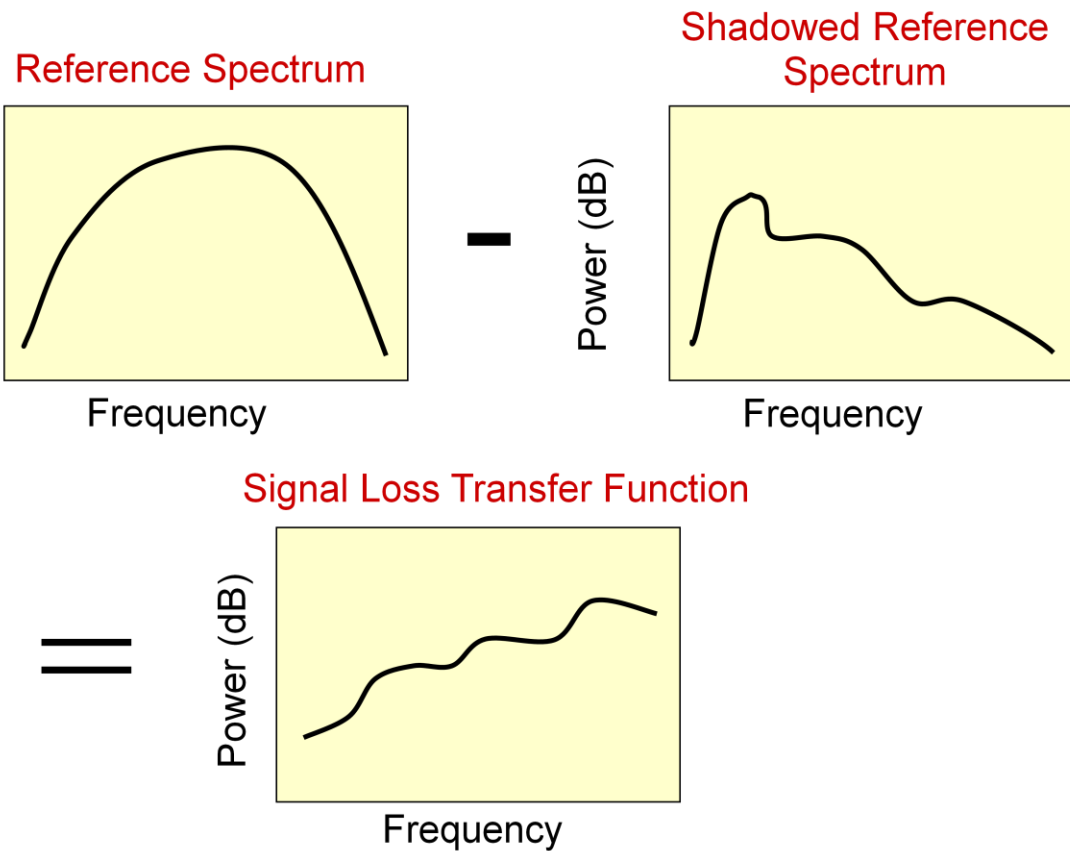
Figure 2.14: To analyze the attenuating effects of the bone as a function of signal frequency, the frequency spectrum of the Shadowed Reference Spectrum is subtracted from the Reference Spectrum to give the Signal Loss Transfer Function, a measure of how much signal is lost as a function of frequency.
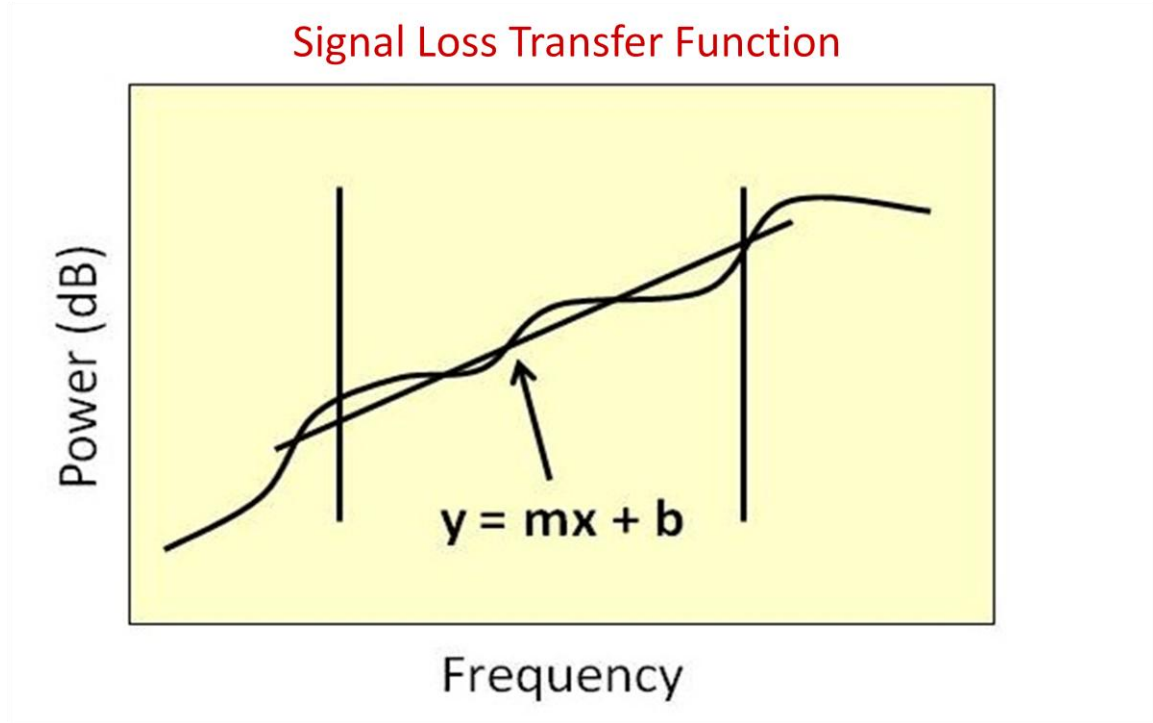
Figure 2.15: The Signal Loss Transfer Function graph is analyzed over a chosen frequency bandwidth. The Frequency Averaged Attenuation, or FAA, is calculated as the averaged power value of the graph over the specified bandwidth divided by twice the specimen thickness, and is measured in dB/cm. The Broadband Ultrasonic Attenuation, or BUA, is the slope of the linear fit ("m" in this image) divided by twice the specimen thickness, measured in dB/(MHz cm).

SECTION 2.7: Determination of Bandwidth

To choose appropriate analysis bandwidths, the -6 dB bandwidths of each set of trials (water backscatter, water attenuation, alcohol backscatter, and alcohol attenuation) were calculated. These bandwidths were found for the calibration and specimen signals for each set of trials. The -6 dB bandwidth represents the frequency values at which each spectrum decreases from the peak power value by 6 dB. This is a standard method for determining the appropriate range of frequency values to analyze in ultrasonic measurements. This process is described below for backscattered signals from water-saturated bone, in Figure 2.16. To determine an appropriate bandwidth for all of the analysis, the specimen spectra for a single set of trials were averaged to get a single

spectrum and the -6 dB bandwidth was found. The -6 dB bandwidth of the calibration

spectra for each trial were also found. The overlap of the -6 dB bandwidths between the

specimen and calibration spectra was chosen as the ultimate bandwidth for analysis of the

signals, shown in Table 2.1.
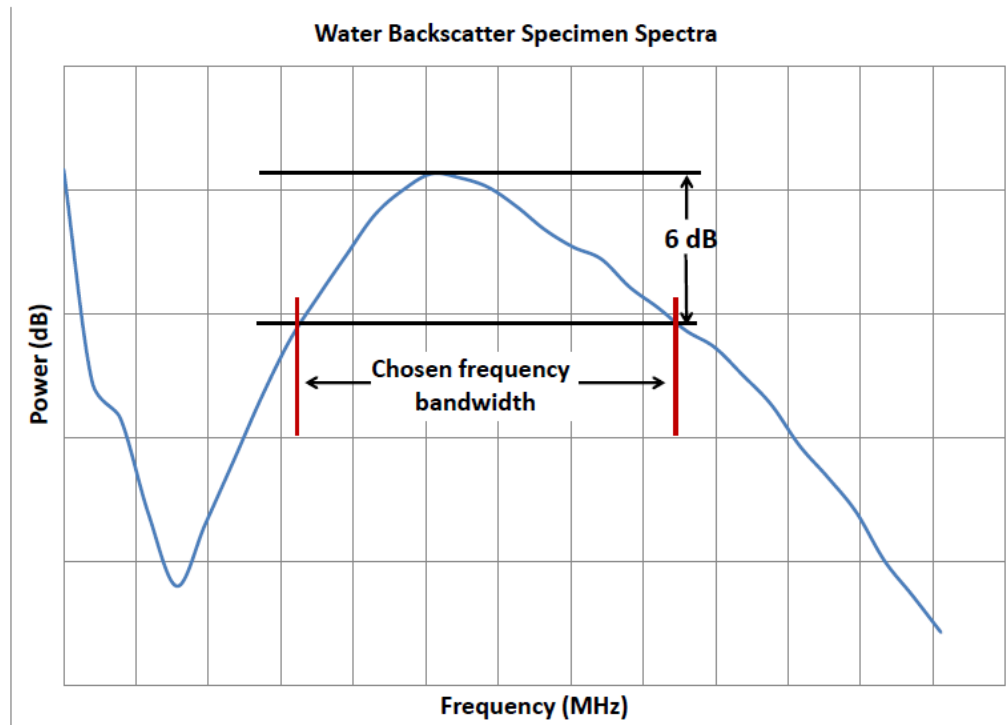
Figure 2.16 (a): To choose the -6dB bandwidth of the specimen signal, the frequency
spectrum of the backscattered signal is analyzed. The points at which the power of the
spectrum drops under 6 dB below the maximum are used to determine the bandwidth.
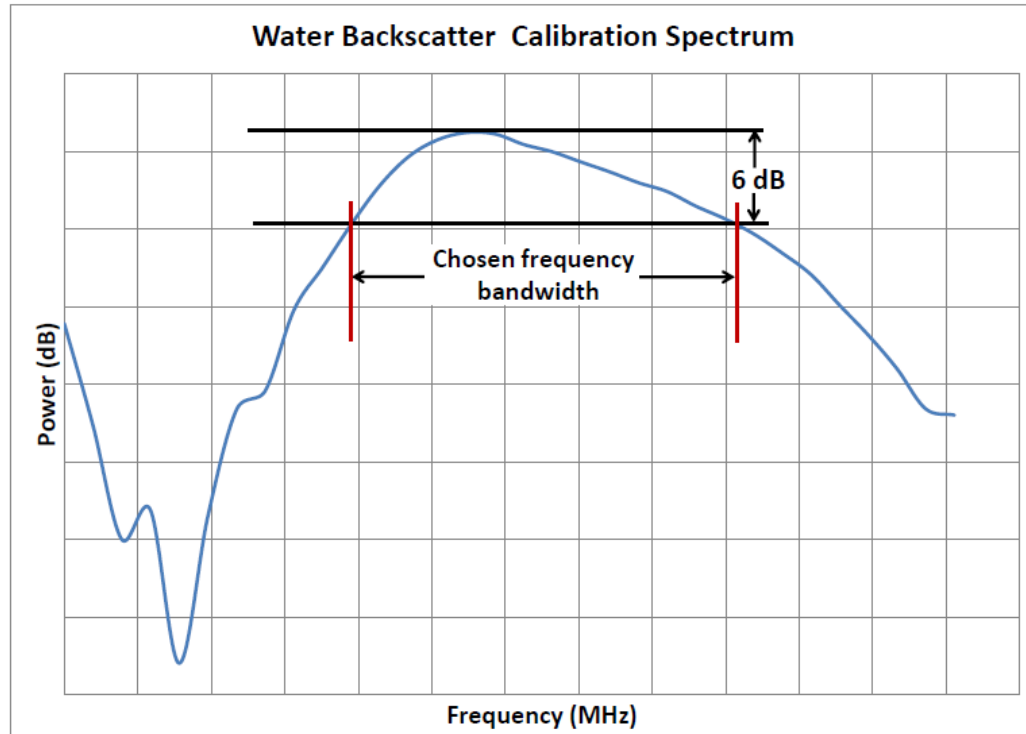
Figure 2.16 (b): To choose the -6dB bandwidth of the reference signal, the frequency spectrum of the reflected signal is analyzed. The points at which the power of the spectrum drops under 6 dB below the maximum are used to determine the bandwidth.

	Specimen Low Frequency (MHz)	Specimen High Frequency (MHz)	Calibration Low Frequency (MHz)	Calibration High Frequency (MHz)	Overlap Minimum (MHz)	Overlap Maximum (MHz)
Backscatter: Water	3.3	8.4	3.9	9	3.9	8.4
Backscatter: Alcohol	3.4	6.8	3.9	7.1	3.9	6.8
Attenuation: Water	1.4	6.2	4	8.6	4	6.2
Attenuation: Alcohol	1.6	5.8	4	7	4	5.8

Table 2.1: The calculated -6 dB bandwidths for each set of trials are shown in this chart, for the specimen and calibration spectra, and then for the ultimate analysis bandwidth, calculated as the overlap of the specimen and calibration overlap.

Chapter 3: Results

SECTION 3.1: Specimen Densities

The range of specimen densities used in this study was 0.142-0.259 g/cc. The distribution of densities are given in Table 3.1 below. The measured values of thickness, length, width, volume, and mass can be found in Appendix A.

Specimen	Density (g/cc)
17C	0.2488
7A	0.1420
7B	0.1833
18C	0.1617
38A	0.1649
38B	0.1584
38C	0.1801
42A	0.2593

Table 3.1: Apparent densities of the specimens used in this study.

SECTION 3.2: Speed of Sound

The average measured speed of sound in water-saturated bone was found to be 1488 ± 11 m/s. The average measured speed of sound in alcohol-saturated bone was found to be 1203 ± 4 m/s. The values of speed of sound in all of the specimens can be found in Appendix B.

SECTION 3.3: Signal Loss Transfer Function

The Signal Loss Transfer Functions (average power lost upon passing through the bone twice as a function of frequency) averaged over all specimens for each trial (Water 1, Water 2, Alcohol 1, Alcohol 2) are shown below, in Figure 3.1. Numerical values are provided in Appendix C.

Specimen Averaged Power Loss Spectra
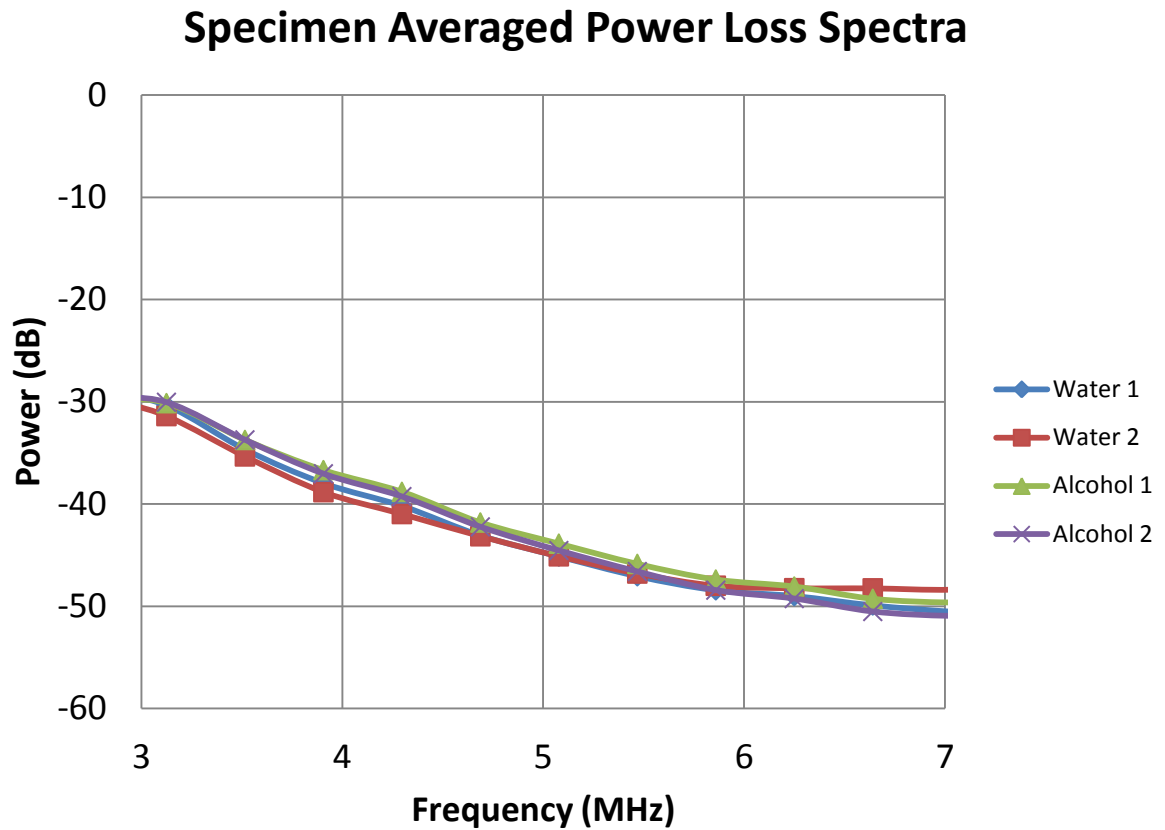
Figure 3.1: A graph of the power loss spectra averaged over all specimens in water and alcohol. The analysis bandwidth in the frequency domain for these signals is 4-6.2 MHz in water and 4-5.8 MHz in alcohol.

SECTION 3.4: Apparent Backscatter Transfer Functions

The apparent backscatter transfer functions (average power backscattered as a function of frequency) averaged over all specimens for each trial (Water 1, Water 2, Alcohol 1, Alcohol 2) are shown below in Figure 3.2. Numerical values are provided in Appendix D.
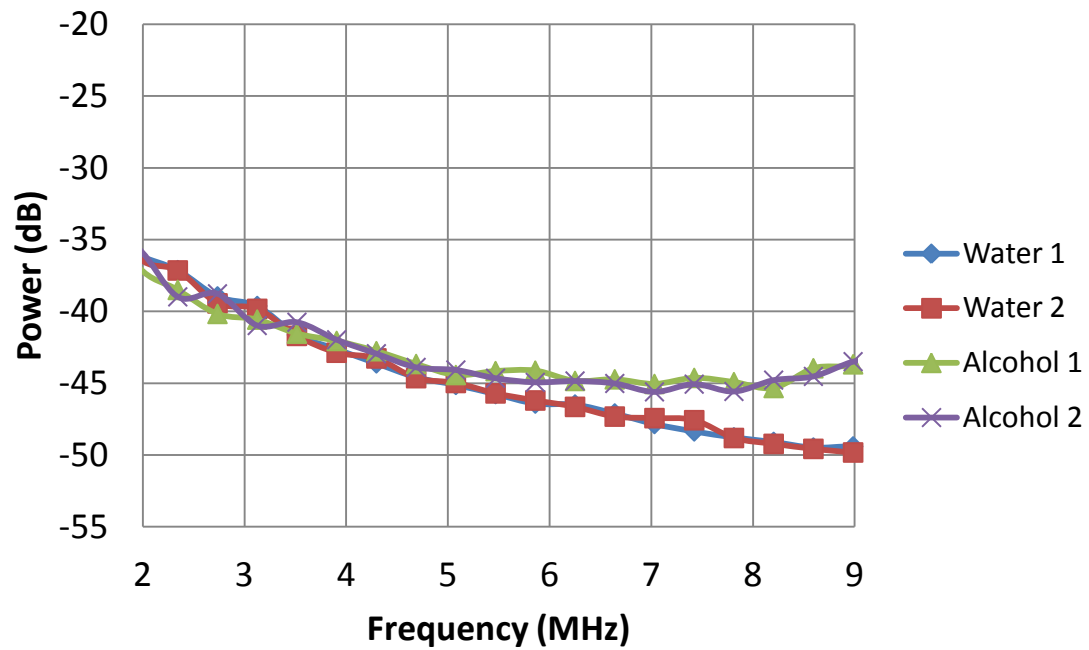
Figure 3.2: A graph of the backscatter spectra averaged over all specimens in water and alcohol. The analysis bandwidth in the frequency domain for these signals is 3.9-8.4 MHz in water and 3.9-6.8 MHz in alcohol.

Chapter 4: Discussion

SECTION 4.1: Signal Loss Transfer Functions

Over the specified (-6 dB) frequency bandwidths, signal power is found to decrease approximately linearly with frequency as seen in Figure 3.2. Frequency Averaged Attenuation (FAA) is measured as the average power lost over the specified frequency range. This value is calculated and divided by the amount of bone that the signal has passed through (in our case, twice the specimen thickness). Units for Frequency Averaged Attenuation are dB/cm. The density dependence of each specimen's attenuation can be seen in the graph of Frequency Averaged Attenuation in Figure 4.1 below.

FAA vs density
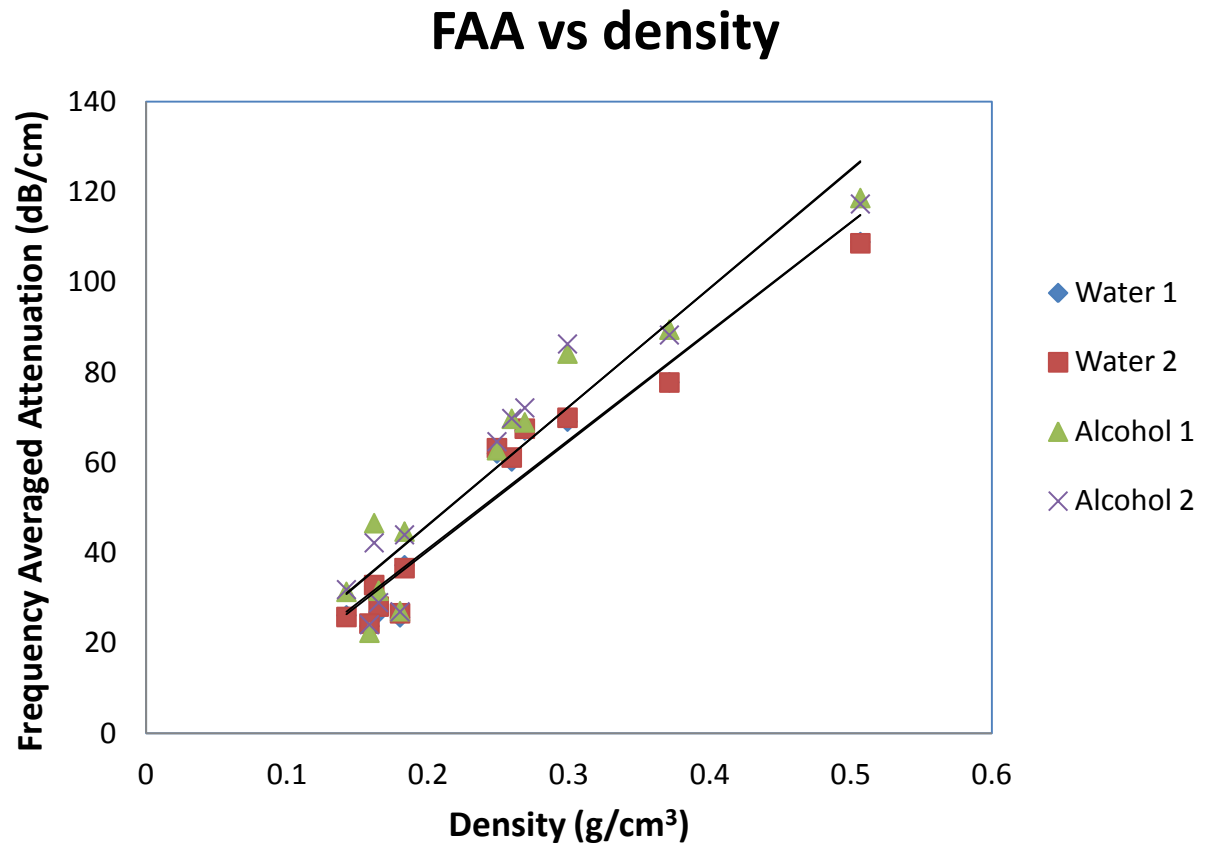
Figure 4.1: The Frequency Averaged Attenuation (dB/cm) for each specimen, averaged over a 50x50 ROI, plotted for each separate trial as a function of Specimen Density (g/cm^3). Correlation coefficients for the linear fits of each trial are as follows: Water 1: R = 0.97, Water 2: R = 0.97, Alcohol 1: R = 0.96, Alcohol 2: R = 0.95.

All four of these trials show a statistically significant (p<0.05) increase of FAA with specimen density. This affirms our previous assumption that the attenuating properties of the bone will increase at higher densities.

SECTION 4.2: Apparent Backscatter Transfer Functions

Over the specified (-6 dB) frequency range for the Apparent Backscatter Transfer Functions, the power scattered back from the interior of the bone specimens decreases approximately linearly with frequency as seen in Figure 3.3. A linear fit is performed on the Apparent Backscatter Transfer Function graphs in the specified frequency bandwidth.

The average power delivered by the backscatter signal over the specified bandwidth is measured as the Apparent Integrated Backscatter (AIB), measured in dB.
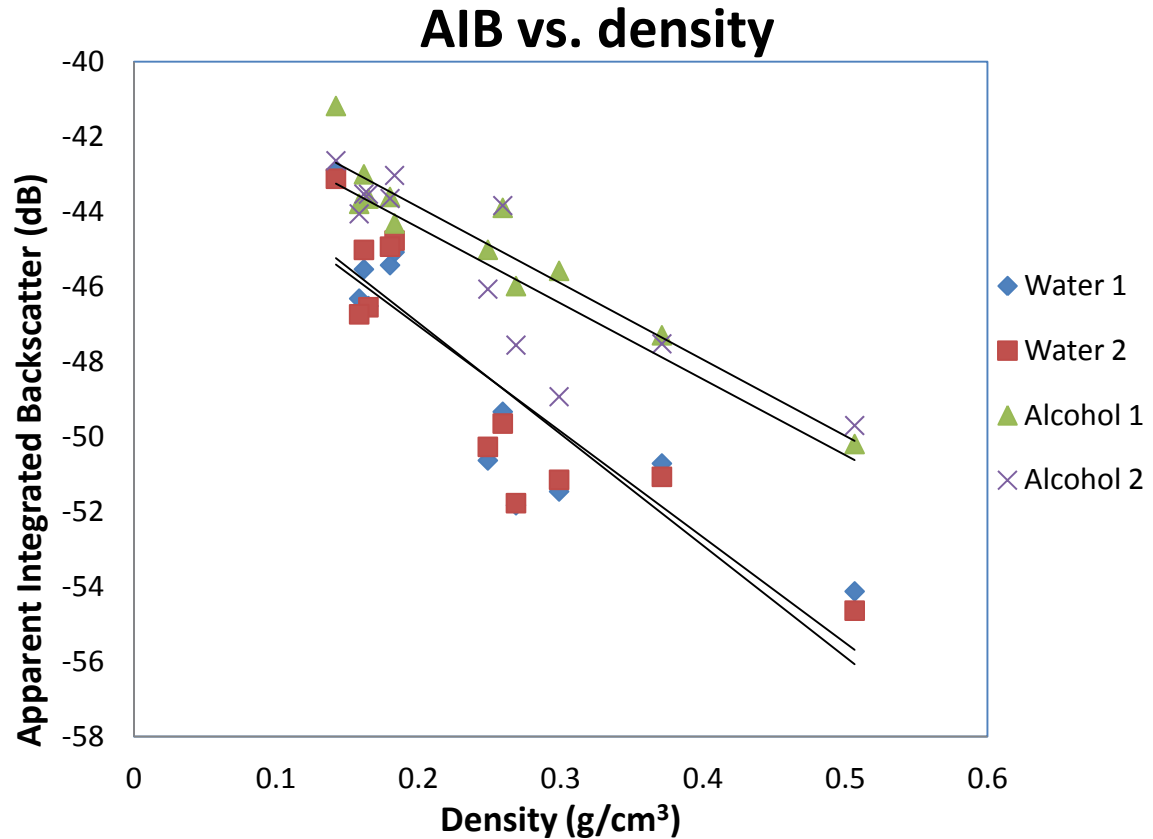
Figure 4.2: The Apparent Integrated Backscatter (dB) values for each specimen, plotted for each separate trial as a function of Specimen Density (g/cm^3). Correlation coefficients for the linear fit of each trial are as follows: Water 1: R = -0.88, Water 2: R = -0.89, Alcohol 1: R = -0.95, Alcohol 2: R = -0.88.

One important thing to note from this graph is that it is consistent with previous results that demonstrate a negative linear correlation between backscattered power and bone density. Also, this graph demonstrates that the backscattered power from the bone saturated in water and alcohol does change, in both overall power and frequency dependence (slope in this graph). These results affirm our assumption that changing the filling fluid of the bone specimens changes the scattering properties of ultrasound in the bone specimen.

SECTION 4.3: Reproducibility of Results

The reproducibility of the results in this experiment was determined by alternating the fluids, to show that the results are consistent and that the properties of the bone are unaltered by changing the filling fluid. One concern was that alcohol may alter the amount or properties of the bony material.

A paired T-test was performed on various combinations of the different trials. In the ABTF data, these tests verified that the trials in water and alcohol were each reproducible (no significant difference between Water 1 and Water 2 or Alcohol 1 and Alcohol 2), but all other combinations showed a statistically significant difference ($p < 0.05$). The SLTF data show no difference between the water trials, but do show a difference for all other combinations of trials ($p < 0.05$). Overall, however, the results appear to be reproducible, and saturating the bone in alcohol does not alter the properties of the bone material.

SECTION 4.4: Effect of Saturating Fluid

An analysis of variance (ANOVA) test was performed on the Apparent Backscatter Transfer Functions and Signal Loss Transfer Functions to determine if there was a statistically significant difference between the trials in water and alcohol. For the ABTF graphs, there was a statistically significant ($p = 0.02$) difference between the four different trials. So, the backscattered properties of the bone have changed as a result of the change of filling fluid. In the SLTF graphs, there was no statistically significant ($p = 0.92$) difference between the different trials. This demonstrates that the attenuating properties of the cancellous bone have not been altered with the change in filling fluid.

The alteration of the saturation fluid in the bone specimens changes the backscatter coefficient of the trabeculae due to the altered acoustic impedance mismatch between the fluid and the trabeculae. The results of this experiment demonstrate that the attenuating properties of the bone specimens does not change with changing saturating fluid of the bone. The higher power backscattered from the alcohol-saturated bone, as evidenced in the Apparent Backscatter Transfer Function graph, is likely due to the higher backscatter coefficient caused by the increased acoustic impedance mismatch between the bone and surrounding fluid. This change can also be seen in the Apparent Integrated Backscatter and Frequency Slope of Apparent Backscatter. The change in filling fluid has indeed altered the scattering properties of the bone as anticipated, as demonstrated by the changed backscatter properties of the bone.

However, despite the changes seen in the scattering properties of the bone, there is no significant different between the attenuating properties of cancellous bone saturated in water and alcohol. Although the scattering of the bone has changed, the attenuation has not. From this information, it can be determined that scattering either plays no role in the measured Signal Loss Transfer Function, or that absorption greatly overshadows the effects of scattering in the signal attenuation. From this, it can be concluded that the dominant mechanism of attenuation in cancellous bone is absorption. Although scattering plays a role in the measured backscattered power, this study concluded that absorption is the dominant mechanism of attenuation of ultrasound in human cancellous bone.

SECTION 4.5: Implications

The relative contributions of scattering and absorption to the attenuating properties of cancellous bone have important implications for the clinical applications of backscattered ultrasound. Our results support our hypothesis that the decrease of Apparent Integrated Backscatter (AIB) with increasing bone density is due to the increased attenuating properties of bone at higher densities. Even more specifically, the increased absorption of bone at higher bone densities causes AIB to decrease with increasing bone density.

This has important implications for applications of backscatter as a method for assessing bone properties. First, we must explore the factors that contribute to scattering and absorption in ultrasonic attenuation. The clinically significant properties of cancellous are its composition and microstructure. Bone composition refers to the mineral and collagen content of the bony material. Bone microstructure of cancellous bone is the geometry of the trabeculae; their size, number, and thickness.

Scattering of ultrasound in cancellous bone is a function of both the bone composition (because this affects the acoustic impedance mismatch between the trabeculae and the surrounding fluid) and the microstructure (the size and shape of the acoustic scatterer). Ultrasonic absorption is mainly a function of the composition of bone and the amount of bony material present; it is relatively insensitive to the specific microstructure or geometry of the bone.

We have determined that attenuation is dominated by the absorbing properties of bone, and that backscattered measurements are strongly influenced by the attenuation of the ultrasonic signal in cancellous bone. Therefore, we can conclude that our

backscattered ultrasonic measurements (specifically, AIB) are largely dependent on the absorbing properties of the bone, and thus the composition of the bone. Backscatter appears to be less sensitive to the microstructure of cancellous bone. This could be further studied by comparing measurements of backscattered ultrasound with the microstructure of bone as determined by micro CT analysis, for example.

This is consistent with previous results that backscatter is more sensitive to changes in collagen content than changes in mineral content. Bone mineral has a large effect on the acoustic impedance of the bony material and collagen has a large effect on the absorption of the bone. The research group found that chemically removing the mineral in the bone did not alter the backscattered power, which should have had a large effect on the contributions of signal scattering to attenuation. In addition, the group found that chemically removing the collagen in the bone had a noticeable effect on the measured backscatter. Since collagen has a significant effect on the absorption properties of the bone, this is also consistent with our results. Backscattered power is heavily influenced by bone attenuation, which is predominantly dependent on the absorption of the ultrasonic signal in the bone (Hoffmeister, Whitten, Kaste, and Rho, 26-32).

Our findings are also significant because models of ultrasonic propagation through cancellous bone have predicted that scattering should be the dominant mechanism at higher frequencies (Kaufman, Luo, and Siffert, 2003). However, we have found the opposite. This suggests that current models of ultrasonic propagation are incorrect or incomplete, and there may be more complicated interactions of the ultrasound with the bone of which we are currently unaware.

Further work could be completed to determine if the changes of bone due to osteoporosis are more significant in the composition or microstructure of bone, and if ultrasound is an effective method of measuring those changes. It is well established that backscattered signal measurements correlate well with the physical density of bone, but there is more nuance in the factors that determine that density that can be explored.

Chapter 5: Conclusions

The goal of this project was to determine the dominant mechanism of attenuation in cancellous bone. Attenuation is known to increase with increasing bone density, and the two mechanisms of attenuation in cancellous bone are absorption and scattering. This study sought to isolate the effects of absorption and scattering by changing the filling fluid of the pores in the bone. Through this, the scattering properties of the bone were altered, but the absorption properties remained constant. There were differences between the backscattered power in water- and alcohol-saturated bone, indicating that the scattering properties of the bone were indeed altered by the changing of the filling fluid. However, there were no changes observed for the attenuation of the bone samples in water and alcohol. From this is can be concluded that absorption is the dominant mechanism of attenuation in cancellous bone.

APPENDIX A

Specimen Density Measurements:

Specimen	7A	7B	18C	38A	38B	38C	42A	17C
Human/Bovine	H	H	H	H	H	H	B	B
T1 (mm)	4.25	4.24	4.31	5	5.07	3.13	3.63	3.14
T2 (mm)	4.37	4.22	3.92	4.98	5.14	2.99	3.67	2.9
T3 (mm)	4.08	4	4.88	4.69	4.72	3.09	3.69	2.82
T4 (mm)	3.94	4.22	4.69	4.92	4.94	3.46	3.6	2.81
T5 (mm)	4.33	4.23	4.64	4.95	4.95	3.48	3.57	2.95
L1 (mm)	14.5	14.16	14.75	14.44	14.96	14.06	15.41	15.22
L2 (mm)	14.41	14.17	14.84	14.22	15.09	14.82	15.43	15.21
L3 (mm)	14.41	13.71	14.81	14.04	14.77	15.07	15.66	15.16
W1 (mm)	14.78	14.74	14.13	14.53	14.72	14.16	15.82	13.77
W2 (mm)	14.75	14.51	14.49	14.39	14.34	13.68	15.81	13.78
W3 (mm)	14.78	13.73	14.21	14.36	14.15	14.05	15.76	13.8
average T (cm)	0.419	0.418	0.449	0.491	0.496	0.323	0.363	0.292
average L (cm)	1.444	1.401	1.480	1.423	1.494	1.465	1.550	1.520
average W (cm)	1.477	1.433	1.428	1.443	1.440	1.396	1.580	1.378
Volume (cm^3)	0.894	0.840	0.948	1.008	1.068	0.661	0.889	0.612
Mass (g)	0.127	0.154	0.153	0.166	0.169	0.119	0.231	0.152
Density (g/cm^3)	0.142	0.183	0.162	0.165	0.158	0.180	0.259	0.249

APPENDIX B

Speed of Sound Measurements:

		Speed of Sound (m/s)			
Specimen	Density	Water 1	Water 2	Alcohol 1	Alcohol 2
17C	0.2488	1484.24	1487.36	1203.39	1208.43
7A	0.1420	1484.29	1484.48	1196.53	1204.41
7B	0.1833	1484.24	1485.61	1195.63	1205.74
18C	0.1617	1484.67	1485.90	1202.9	1206.56
38A	0.1649	1487.73	1486.43	1199.8	1198.72
38B	0.1584	1484.31	1484.10	1204.84	1202.14
38C	0.1800	1486.01	1487.07	1203.42	1205.55
42A	0.2593	1486.69	1486.73	1205.60	1203.14

APPENDIX C:

Signal Loss Transfer Functions:
Water 1:

Orientation:	Lateral	Medial	Lateral	Medial
Specimen:	17C	17C	7A	7A
Frequency (MHz)				
4.2969	-43.413	-43.930	-31.172	-31.401
4.6875	-44.847	-45.600	-34.681	-34.695
5.0781	-45.281	-47.040	-37.342	-37.309
5.4688	-46.980	-48.589	-39.590	-39.814
5.8594	-48.198	-50.720	-41.596	-41.743

Orientation:	Lateral	Medial	Lateral	Medial
Specimen:	7B	7B	18C	18C
Frequency (MHz)				
4.2969	-42.519	-39.808	-42.021	-41.868
4.6875	-45.567	-44.445	-45.440	-45.553
5.0781	-47.768	-45.291	-47.824	-47.607
5.4688	-51.271	-46.825	-49.381	-49.579
5.8594	-52.389	-48.587	-51.142	-52.107

Orientation:	Lateral	Medial	Lateral	Medial
Specimen:	38A	38A	38B	38B
Frequency (MHz)				
4.2969	-36.893	-35.762	-34.038	-34.500
4.6875	-37.632	-39.539	-38.217	-36.701
5.0781	-40.931	-41.120	-40.401	-38.467
5.4688	-42.966	-43.447	-42.097	-39.932
5.8594	-43.515	-44.435	-42.451	-41.804

Orientation:	Lateral	Medial	Lateral	Medial
Specimen:	38C	38C	42A	42A
Frequency (MHz)				
4.2969	-26.591	-26.705	-66.420	-66.202
4.6875	-28.665	-28.943	-70.300	-68.669
5.0781	-29.909	-29.702	-74.539	-71.693
5.4688	-31.359	-30.811	-75.814	-74.646
5.8594	-32.141	-31.945	-76.167	-76.148

Water 2:

Orientation:	Lateral	Medial	Lateral	Medial
Specimen:	17C	17C	7A	7A
Frequency (MHz)				
4.2969	-43.662	-42.765	-31.321	-31.666
4.6875	-44.665	-43.487	-34.423	-34.614
5.0781	-44.872	-43.424	-37.440	-37.249
5.4688	-45.794	-43.524	-39.410	-39.710
5.8594	-46.339	-44.041	-40.801	-41.571

Orientation:	Lateral	Medial	Lateral	Medial
Specimen:	7B	7B	18C	18C
Frequency (MHz)				
4.2969	-41.925	-42.623	-40.905	-41.400
4.6875	-44.072	-43.944	-44.652	-44.415
5.0781	-46.957	-46.427	-46.196	-46.564
5.4688	-48.934	-48.155	-49.003	-48.366
5.8594	-50.613	-49.443	-50.790	-49.802

Orientation:	Lateral	Medial	Lateral	Medial
Specimen:	38A	38A	38B	38B
Frequency (MHz)				
4.2969	-38.817	-40.225	-37.949	-35.252
4.6875	-38.975	-41.683	-38.846	-36.613
5.0781	-42.080	-45.381	-40.549	-38.992
5.4688	-43.208	-46.182	-42.449	-40.680
5.8594	-43.984	-47.115	-44.502	-42.344

Orientation:	Lateral	Medial	Lateral	Medial
Specimen:	38C	38C	42A	42A
Frequency (MHz)				
4.2969	-27.601	-27.111	-66.229	-66.348
4.6875	-29.763	-29.240	-71.321	-69.834
5.0781	-30.414	-30.220	-73.828	-71.316
5.4688	-31.318	-31.303	-76.071	-74.770
5.8594	-32.703	-31.913	-75.824	-76.255

Alcohol 1:

Orientation:	Lateral	Medial	Lateral	Medial
Specimen:	17C	17C	7A	7A
Frequency (MHz)				
4.2969	-41.036	-39.012	-31.034	-31.572
4.6875	-44.344	-43.016	-33.744	-34.437
5.0781	-46.538	-45.213	-36.363	-36.983
5.4688	-47.740	-46.590	-38.981	-38.560
5.8594	-50.703	-48.788	-41.366	-41.058

Orientation:	Lateral	Medial	Lateral	Medial
Specimen:	7B	7B	18C	18C
Frequency (MHz)				
4.2969	-40.314	-43.8756	-45.199	-42.311
4.6875	-43.308	-46.999	-48.290	-46.497
5.0781	-46.361	-48.751	-50.033	-48.443
5.4688	-49.092	-51.275	-50.751	-51.665
5.8594	-51.195	-52.995	-51.951	-51.513

Orientation:	Lateral	Medial	Lateral	Medial
Specimen:	38A	38A	38B	38B
Frequency (MHz)				
4.2969	-35.180	-36.768	-30.381	-28.013
4.6875	-37.976	-39.953	-32.983	-29.569
5.0781	-41.073	-41.642	-35.331	-31.923
5.4688	-40.988	-43.498	-37.462	-33.427
5.8594	-42.626	-44.895	-38.288	-34.864

Orientation:	Lateral	Medial	Lateral	Medial
Specimen:	38C	38C	42A	42A
Frequency (MHz)				
4.2969	-23.845	-23.701	-63.293	-65.581
4.6875	-25.530	-25.594	-67.533	-69.324
5.0781	-26.836	-26.906	-70.917	-68.866
5.4688	-28.487	-28.602	-72.3670	-74.381
5.8594	-30.251	-30.171	-72.221	-75.458

Alcohol 2:

Orientation:	Lateral	Medial	Lateral	Medial
Specimen:	17C	17C	7A	7A
Frequency (MHz)				
4.2969	-44.701	-41.302	-31.908	-31.161
4.6875	-48.200	-45.254	-35.280	-34.197
5.0781	-49.382	-47.668	-37.571	-36.492
5.4688	-49.993	-50.553	-40.267	-38.599
5.8594	-50.931	-52.411	-42.998	-40.961

Orientation:	Lateral	Medial	Lateral	Medial
Specimen:	7B	7B	18C	18C
Frequency (MHz)				
4.2969	-40.170	-43.928	-44.664	-43.185
4.6875	-42.827	-45.871	-48.249	-47.667
5.0781	-46.741	-49.508	-50.677	-50.054
5.4688	-49.718	-51.400	-53.644	-52.098
5.8594	-51.787	-52.756	-56.933	-53.293

Orientation:	Lateral	Medial	Lateral	Medial
Specimen:	38A	38A	38B	38B
Frequency (MHz)				
4.2969	-35.216	-34.279	-31.876	-29.171
4.6875	-38.037	-37.387	-34.300	-31.404
5.0781	-40.265	-39.755	-36.750	-33.350
5.4688	-42.219	-41.481	-39.206	-35.236
5.8594	-43.990	-42.352	-41.168	-37.187

Orientation:	Lateral	Medial	Lateral	Medial
Specimen:	38C	38C	42A	42A
Frequency (MHz)				
4.2969	-22.971	-23.679	-63.329	-66.947
4.6875	-24.859	-25.689	-66.946	-69.715
5.0781	-26.080	-27.408	-70.269	-70.954
5.4688	-27.436	-28.375	-72.224	-73.322
5.8594	-29.048	-29.779	-73.771	-75.602

APPENDIX D:

Apparent Backscatter Transfer Functions:
Water 1:

Orientation:	Lateral	Medial	Lateral	Medial
Specimen:	17C	17C	7A	7A
Frequency (MHz)				
4.2969	-46.736	-44.950	-41.517	-41.970
4.6875	-49.554	-47.630	-43.247	-40.098
5.0781	-50.167	-48.995	-42.335	-40.659
5.4688	-49.891	-49.551	-40.440	-41.735
5.8594	-51.464	-47.434	-41.223	-42.915
6.25	-51.007	-49.635	-41.683	-43.141
6.6406	-51.832	-50.977	-41.290	-45.549

Orientation:	Lateral	Medial	Lateral	Medial
Specimen:	7B	7B	18C	18C
Frequency (MHz)				
4.2969	-39.849	-42.398	-43.893	-41.661
4.6875	-40.477	-45.307	-44.714	-43.525
5.0781	-40.306	-44.076	-46.068	-44.297
5.4688	-41.745	-46.659	-46.003	-44.039
5.8594	-43.947	-47.900	-46.728	-44.107
6.25	-44.044	-46.537	-47.112	-44.485
6.6406	-43.245	-48.259	-48.542	-45.171

Orientation:	Lateral	Medial	Lateral	Medial
Specimen:	18C	18C	38A	38A
Frequency (MHz)				
4.2969	-43.893	-41.661	-43.957	-45.280
4.6875	-44.714	-43.525	-43.601	-48.148
5.0781	-46.068	-44.297	-43.556	-48.212
5.4688	-46.003	-44.039	-45.164	-49.461
5.8594	-46.728	-44.107	-44.773	-47.288
6.25	-47.112	-44.485	-44.367	-47.386
6.6406	-48.542	-45.171	-44.842	-48.214

Orientation:	Lateral	Medial	Lateral	Medial
Specimen:	38C	38C	42A	42A
Frequency (MHz)				
4.2969	-42.389	-44.225	-42.244	-48.589
4.6875	-42.164	-46.139	-42.690	-48.951
5.0781	-43.496	-46.224	-44.450	-47.252
5.4688	-44.702	-46.475	-44.843	-49.797
5.8594	-44.922	-48.836	-46.134	-51.564
6.25	-44.229	-47.541	-47.776	-50.897
6.6406	-43.750	-47.989	-47.839	-51.965

Water 2:

Orientation:	Lateral	Medial	Lateral	Medial
Specimen:	17C	17C	7A	7A
Frequency (MHz)				
4.2969	-48.005	-46.469	-41.997	-39.637
4.6875	-49.039	-49.327	-41.986	-41.767
5.0781	-48.176	-47.636	-43.769	-40.005
5.4688	-49.379	-48.919	-40.918	-41.542
5.8594	-48.286	-51.187	-41.612	-42.975
6.25	-50.356	-48.219	-45.637	-43.598
6.6406	-50.153	-49.955	-44.935	-43.385

Orientation:	Lateral	Medial	Lateral	Medial
Specimen:	7B	7B	18C	18C
Frequency (MHz)				
4.2969	-38.736	-43.409	-40.440	-43.421
4.6875	-41.249	-44.497	-42.785	-44.652
5.0781	-40.321	-44.525	-43.177	-46.438
5.4688	-40.961	-45.796	-43.744	-46.094
5.8594	-41.411	-45.700	-43.969	-46.235
6.25	-42.937	-46.282	-43.764	-47.127
6.6406	-43.513	-48.542	-44.908	-48.503

Orientation:	Lateral	Medial	Lateral	Medial
Specimen:	38A	38A	38B	38B
Frequency (MHz)				
4.2969	-44.200	-42.543	-43.882	-42.749
4.6875	-45.633	-44.443	-44.198	-44.691
5.0781	-45.158	-44.474	-46.506	-46.994
5.4688	-46.909	-46.694	-46.367	-47.997
5.8594	-47.001	-46.332	-47.216	-47.633
6.25	-46.625	-46.402	-46.517	-47.950
6.6406	-47.449	-48.110	-45.763	-49.644

Orientation:	Lateral	Medial	Lateral	Medial
Specimen:	38C	38C	42A	42A
Frequency (MHz)				
4.2969	-43.103	-42.624	-42.083	-49.030
4.6875	-45.723	-41.017	-42.867	-50.424
5.0781	-46.429	-42.965	-44.874	-48.240
5.4688	-46.763	-44.223	-44.709	-50.281
5.8594	-48.041	-42.323	-47.48	-51.806
6.25	-47.897	-42.781	-47.775	-52.473
6.6406	-47.264	-42.798	-48.992	-53.248

Alcohol 1:

Orientation:	Lateral	Medial	Lateral	Medial
Specimen:	17C	17C	7A	7A
Frequency (MHz)				
4.2969	-43.618	-43.910	-39.884	-40.041
4.6875	-45.979	-44.814	-43.025	-40.859
5.0781	-46.981	-45.266	-42.891	-41.887
5.4688	-45.598	-47.513	-41.475	-42.227
5.8594	-44.336	-47.424	-40.164	-44.882
6.25	-46.840	-49.294	-42.123	-42.608
6.6406	-47.453	-46.759	-42.681	-40.603

Orientation:	Lateral	Medial	Lateral	Medial
Specimen:	7B	7B	18C	18C
Frequency (MHz)				
4.2969	-48.378	-43.496	-41.142	-43.104
4.6875	-45.309	-41.410	-43.325	-45.344
5.0781	-44.425	-45.159	-43.695	-44.855
5.4688	-45.348	-43.252	-46.296	-43.750
5.8594	-43.365	-43.908	-45.770	-44.893
6.25	-45.159	-43.127	-43.758	-44.656
6.6406	-44.937	-45.463	-41.906	-44.526

Orientation:	Lateral	Medial	Lateral	Medial
Specimen:	38A	38A	38B	38B
Frequency (MHz)				
4.2969	-43.556	-40.982	-43.764	-42.317
4.6875	-43.244	-42.069	-44.108	-42.396
5.0781	-43.849	-45.162	-42.996	-45.201
5.4688	-42.349	-43.554	-42.199	-43.419
5.8594	-42.487	-43.607	-43.112	-42.553
6.25	-44.167	-44.576	-44.793	-43.594
6.6406	-44.254	-44.887	-44.597	-44.497

Orientation:	Lateral	Medial	Lateral	Medial
Specimen:	38C	38C	42A	42A
Frequency (MHz)				
4.2969	-42.220	-40.994	-41.7867	-45.0802
4.6875	-43.269	-43.992	-44.983	-44.439
5.0781	-42.255	-44.108	-44.697	-47.420
5.4688	-42.584	-45.147	-44.772	-47.013
5.8594	-42.817	-44.776	-43.800	-48.103
6.25	-44.495	-44.142	-45.272	-48.820
6.6406	-43.530	-44.721	-45.151	-49.663

Alcohol 2:

Orientation:	Lateral	Medial	Lateral	Medial
Specimen:	17C	17C	7A	7A
Frequency (MHz)				
4.2969	-44.270	-43.570	-42.515	-40.673
4.6875	-48.907	-46.665	-44.690	-42.527
5.0781	-46.401	-44.461	-42.865	-43.294
5.4688	-47.638	-48.235	-44.933	-40.306
5.8594	-47.488	-47.741	-44.355	-43.666
6.25	-47.226	-47.849	-42.417	-43.247
6.6406	-49.784	-48.324	-44.031	-42.610

Orientation:	Lateral	Medial	Lateral	Medial
Specimen:	7B	7B	18C	18C
Frequency (MHz)				
4.2969	-42.844	-41.369	-44.190	-40.877
4.6875	-41.638	-42.701	-45.483	-42.805
5.0781	-44.843	-41.370	-44.573	-43.235
5.4688	-40.511	-41.154	-44.941	-46.196
5.8594	-43.793	-44.047	-45.262	-44.940
6.25	-42.725	-43.685	-43.930	-44.364
6.6406	-44.514	-43.388	-44.704	-45.000

Orientation:	Lateral	Medial	Lateral	Medial
Specimen:	38A	38A	38B	38B
Frequency (MHz)				
4.2969	-44.992	-42.654	-43.802	-42.207
4.6875	-42.748	-44.306	-45.119	-43.158
5.0781	-45.496	-43.359	-43.282	-43.502
5.4688	-43.554	-45.139	-43.904	-45.684
5.8594	-43.075	-42.646	-45.186	-43.552
6.25	-43.954	-43.911	-45.158	-44.140
6.6406	-43.485	-44.423	-44.449	-44.300

Orientation:	Lateral	Medial	Lateral	Medial
Specimen:	38C	38C	42A	42A
Frequency (MHz)				
4.2969	-42.282	-43.310	-41.323	-46.171
4.6875	-39.882	-42.037	-42.150	-47.498
5.0781	-43.023	-44.867	-43.798	-46.853
5.4688	-41.766	-47.083	-46.116	-47.246
5.8594	-43.434	-46.532	-45.284	-47.963
6.25	-42.717	-46.637	-45.753	-49.747
6.6406	-41.626	-46.909	-44.498	-48.213

Bibliography

"Barrington Orthopedic Specialists and Sports Medicine - Barrington Orthopedic Specialists." *Barrington Orthopedic Specialists and Sports Medicine - Barrington Orthopedic Specialists*. Web. <http://www.barringtonortho.com/>.

"Bone 2: Compact and Spongy Bone." *University of Glasgow*. Web. <http://www.gla.ac.uk/ibls/US/fab/tutorial/generic/bone2.html>.

"CT Scan." *Glossary: , Masonic Cancer Center, University of Minnesota*. Web. <http://www.cancer.umn.edu/cancerinfo/NCI/glossary/CDR46033.html>.

Chaffai S and V. Roberjot, "Frequency dependence of ultrasonic backscattering in cancellous bone: Autocorrelation model and experimental results", *J. Acoust. Soc. Am*. Volume 108, Issue 5: 2403-2411 (2000).

Hoffmeister BK, Johnson DP, Janeski JA, Keedy DA, Steinert BW, Viano AM and Kaste SC, "Ultrasonic characterization of human cancellous bone in vitro using three different apparent backscatter parameters in the frequency range 0.6-15.0 MHz," *IEEE Transactions on Ultrasonics, Ferroelectrics, and Frequency Control*, 55(7), 1442-1452 (2008).

Hoffmeister BK, Jones CI III, Caldwell GJ and Kaste SC, "Ultrasonic characterization of cancellous bone using apparent integrated backscatter," *Physics in Medicine and Biology*, 51, 2715-2727 (2006).

Hoffmeister BK, SA Whitten, and JY Rho, "Low megahertz ultrasonic properties of bovine cancellous bone," *Bone*, vol. 26, pp. 635-642 (2000).

Kaufman, Jonathan J., Gangming Luo, and Robert S. Siffert "On the relative contributions of absorption and scattering to ultrasound attenuation in trabecular bone: A simulation study", *2003 IEEE Symposium on Ultrasonics* 2: 1519-1523 (2003).

Khasanshin, T.S. and A.A. Aleksandrov, "Thermodynamic Properties of Ethanol at Atmospheric Pressure" *J Eng Phys* 47: 1046-1052; (1984).

Lee, Kang Il, Min Joo Choi, "Frequency-dependent attenuation and backscatter coefficients in bovine trabecular bone from 0.2 to 1.2 MHz", *J. Acoust. Soc. Am*. 131(1): EL67-EL73 (2011).

"Mark A. Wolgin, MD Orthopaedic Surgeon." *Osteoporosis*. Web. <http://drwolgin.com/osteoporosis.aspx>.

Njeh, Christopher F., Xiao Guang Cheng, J Mark Elliot, and Pierre J. Meunier. "Bone, Bone Diseases and Bone Quality." *Quantitative Ultrasound: Assessment of Osteoporosis and Bone Status*. By London: Martin Dunitz, 1999. 1-20. Print.

"Osteoporosis Screening Services - CUBACLINICAL ULTRASOUND SCAN." *Osteoporosis Screening Services*. Web. <http://osteoporosisscreeningservice.com/page3.htm>.

Slutsky, L.J. "Ultrasonic chemical relaxation spectroscopy" *Methods of Experimental Physics*, Vol. 19: 179-235; (1981).

Wear, Keith A. "Anisotropy of ultrasonic backscatter and attenuation from human calcaneus: Implications for relative roles of absorption and scattering in determining attenuation", *J Acoust Soc Am*. 107(6): 3474-3479 (2000).